Tectonophysics 460 (2008) 55–75

Contents lists available at ScienceDirect

Tectonophysics

journal homepage: www.elsevier.com/locate/tecto

Crustal structure at the easternmost termination of the Variscan belt based on CELEBRATION 2000 and ALP 2002 data

P. Hrubcová [a,*], P. Środa [b]
CELEBRATION 2000 Working Group [1]

[a] Institute of Geophysics, Academy of Sciences of the Czech Republic, Prague, Czech Republic
[b] Institute of Geophysics, Polish Academy of Sciences, Warsaw, Poland

ARTICLE INFO

Article history:
Received 28 November 2006
Received in revised form 23 June 2008
Accepted 2 July 2008
Available online 18 July 2008

Keywords:
Variscan orogen
Bohemian Massif
Crustal structure
Refraction and wide-angle reflection
Seismic methods

ABSTRACT

The eastern margin of the Variscan belt in Europe comprises plate boundaries between continental blocks and terranes formed during different tectonic events. The crustal structure of that complicated area was studied using the data of the international refraction experiments CELEBRATION 2000 and ALP 2002. The seismic data were acquired along SW–NE oriented refraction and wide-angle reflection profiles CEL10 and ALP04 starting in the Eastern Alps, passing through the Moravo-Silesian zone of the Bohemian Massif and the Fore-Sudetic Monocline, and terminating in the TESZ in Poland. The data were interpreted by seismic tomographic inversion and by 2-D trial-and-error forward modelling of the P waves. Velocity models determine different types of the crust–mantle transition, reflecting variable crustal thickness and delimiting contacts of tectonic units in depth. In the Alpine area, few km thick LVZ with the Vp of 5.1 km s^{-1} dipping to the SW and outcropping at the surface represents the Molasse and Helvetic Flysch sediments overthrust by the Northern Calcareous Alps with higher velocities. In the Bohemian Massif, lower velocities in the range of 5.0–5.6 km s^{-1} down to a depth of 5 km might represent the SE termination of the Elbe Fault Zone. The Fore-Sudetic Monocline and the TESZ are covered by sediments with the velocities in the range of 3.6–5.5 km s^{-1} to the maximum depth of 15 km beneath the Mid-Polish Trough. The Moho in the Eastern Alps is dipping to the SW reaching the depth of 43–45 km. The lower crust at the eastern margin of the Bohemian Massif is characterized by elevated velocities and high Vp gradient, which seems to be a characteristic feature of the Moravo-Silesian. Slightly different properties in the Moravian and Silesian units might be attributed to varying distances of the profile from the Moldanubian Thrust front as well as a different type of contact of the Brunia with the Moldanubian and its northern root sector. The Moho beneath the Fore-Sudetic Monocline is the most pronounced and is interpreted as the first-order discontinuity at a depth of 30 km.

1. Introduction

The tectonic evolution of the Variscan orogenic belt is related to amalgamation of various continental crustal blocks previously situated between Baltica in the NE and Gondwana in the SW during the Devonian and Late Carboniferous (Matte et al., 1990). This belt is characterized by the Ibero-Armorican spread from north Africa to the Bohemian Massif in central Europe.

The eastern termination of the Variscan belt comprises plate boundaries between continental blocks and terranes formed during different tectonic events. Its south-eastern margin was influenced and modified by large movements between Africa and Europe resulting in the Alpine deformation. On the other hand, the north-eastern termination of the Variscan orogen is obliquely cut off and offset by large transcurrent dextral faults parallel with the TESZ (like the Elbe zone or the Odra Fault zone) considered by some authors as forming the southern boundary of the East European Craton (e.g., Dallmeyer et al., 1995; Winchester et al., 2002; Dadlez et al., 2005). The nature and position of boundaries between these units have been interpreted by several investigators, sometimes controversially (e.g. Matte et al., 1990; Fritz et al., 1996; Schulmann and Gayer, 2000; Edel et al., 2003) and are still a matter of ongoing debates. Recent ideas about tectonic history of Central European Variscides have been presented by e.g. Winchester et al. (2006) and Franke (2006).

The Variscan Belt as a prominent structure in Europe has been subject of a vast amount of geophysical investigations and interpretations

* Corresponding author.
E-mail address: pavla@ig.cas.cz (P. Hrubcová).
[1] Celebration 2000 Working Group: A. Guterch[a], M. Grad[b], T. Janik[a], G.R. Keller[c], E. Hegedüs[d], J. Vozár[e], A. Špičák[f], E. Brückl[g], H. Thybo[h]. [a]Institute of Geophysics, Polish Academy of Sciences, Poland. [b]Institute of Geophysics, University of Warsaw, Poland. [c]Department of Geological Sciences, University of Texas at El Paso, USA. [d]Eötvös Loránd Geophysical Institute, Budapest, Hungary. [e]Geological Survey, Bratislava, Slovak Republic. [f]Geophysical Institute Academy of Sciences, Prague, Czech Republic. [g]Vienna University of Technology, Austria. [h]University of Copenhagen, Denmark.

0040-1951/$ – see front matter © 2008 Elsevier B.V. All rights reserved.
doi:10.1016/j.tecto.2008.07.009

over decades. Starting in Iberia (Simancas et al., 2003; Carbonell et al., 2004), through western to central Europe (British Institutions Reflection Profiling Syndicate (BIRPS) and Étude Continentale et Océanique par Réflexion et Refraction (ECORS), 1986; Deutches Kontinentales Reflektionsseismisches Programm (DEKORP) Research Group, 1985, 1988; Aichroth et al., 1992; Onken et al., 2000) it includes also the CELEBRATION 2000 and SUDETES 2003 experiments at its eastern termination (Guterch et al., 2003; Grad et al., 2003b). The EUROPROBE project (Gee and Zeyen, 1996), investigating evolution of the European lithosphere, targeted also the Variscan areas.

The most eastern part of the Variscan orogen is constituted of the Bohemian Massif, a large stable outcrop of pre-Permian rocks. Eastern sectors of the Bohemian Massif comprise the Moldanubian and the Moravo-Silesian zones, the last one having a completely different tectonic history as a part of a separate micro-continent (e.g. Winchester et al., 2002). The development in this region is a result of oblique collision between the Moldanubian terrane and the Brunovistulian micro-continent to the east (Dudek, 1980), where the Moldanubian is viewed as a Variscan orogenic root thrust over the Brunovistulian forming together the Moravo-Silesian zone (Matte, 1991; Schulmann et al., 2005).

The Moravo-Silesian zone is an appropriate area to study tectonic development due to a superposition of three structural levels corresponding to three orogenic cycles (e.g., Grygar et al., 2002). The lowermost cycle represents the Pan-African (Cadomian) Brunovistulian foreland terrane, which determined and influenced complex geological development of the second cycle, the Variscan accretion wedge, represented by volcano-sedimentary formations of the Rhenohercynian foredeep and the Sub-Variscan foreland. Finally, sequences of the West Carpathian foredeep and the Outer West Carpathian nappes formed the Alpine accretion wedge. The Brunovistulicum is the oldest crustal segment and represents a foreland of both the above-mentioned accretionary wedges: the older Variscan one with generally NE directed kinematics and the younger Alpine wedge with northward tectonics. The goal of this study includes supplying answers on the crustal and upper mantle structure of this area together with delimitation of the contact with the Eastern Alps and the north-eastern continuation of the Brunovistulian beneath the Fore-Sudetic Monocline and the TESZ.

To investigate the area, we are using refraction and wide-angle reflection data along the CEL10 profile from CELEBRATION 2000 experiment (Guterch et al., 2003) and ALP04 profile of the ALP 2002 experiment (Brückl et al., 2003). The SW–NE orientated line of joint profiles CEL10 and ALP04 starts in the Central to Eastern Alps, continues along the eastern edge of the Bohemian Massif and ends at the Mid-Polish Trough (MPT) — a part of the Trans-European Suture Zone (TESZ) forming the SW margin of the East European Craton (see Fig. 1). For the interpretation, we choose the tomographic inversion routine of Hole (1992) as a tool to determine a preliminary model of seismic P-wave velocity in the crust using first arrivals. The resulting tomographic model is further improved by two-dimensional (2-D) trial-and-error forward modelling of the refracted and reflected P waves using a ray-tracing algorithm (Červený and Pšenčík, 1984). In this study, we concentrate on velocity variations along the profile; azimuthal anisotropic studies are a matter of other investigations (e.g., Plomerová et al., 1984; Růžek et al., 2003; Vavryčuk et al., 2004).

2. Geology and tectonic evolution of the region

The easternmost termination of the Variscan belt in central Europe comprises the Bohemian Massif, which developed approximately between 480 and 290 Ma (Matte, 2001) and played an important role in the development of the Variscan orogen. At the eastern margin of the Bohemian Massif, the Moldanubian root was thrust over the Brunovistulian foreland along a major dextral transpressional zone during the imbrication of the Brunovistulian, forming the Moravo-Silesian zone (Fritz et al., 1996). The Moravo-Silesian is a 50 km wide and 300 km long NE–SW-trending zone of sheared and metamorphosed Brunia-derived rocks and represents an interface between the upper Moldanubian terrane and the undeformed rocks of the Brunovistulian foreland covered by Devonian to Carboniferous sediments (Schulmann and Gayer, 2000) (see Fig. 1).

The Moravo-Silesian zone of the Bohemian Massif can be followed from Krems in Austria to the NE, where it is often thought to extend to the Odra Fault Zone (OFZ) in Poland. The northern termination of the Moravo-Silesian zone is still not well recognized and is a matter of debates (e.g. Matte, 1986). In this part, the external belt of the Variscan orogen extends beneath the Fore-Sudetic Monocline and continues to the presumed assemblage of suspect terranes accreted to Baltica in the Early Paleozoic called the Trans-European Suture Zone (TESZ) (Berthelsen, 1992; Dadlez et al., 2005). To the SE, the Cadomian Brunia continent submerges beneath the Carpathian Foredeep and the Outer Carpathians, where it may form a basement reactivated during the Alpine orogen (Dallmeyer and Urban, 1994; Fritz et al., 1996). To the south, the belt was influenced by the Alpine orogen, when the Alpine nappes were thrust northwards onto the European foreland including the Bohemian Massif. Most of the basement of the Eastern Alps corresponds to the internal parts of the Variscan belt.

The Moravo-Silesian zone can be divided into two parts — the southern and northern segments referred to as the Moravian and Silesian units, respectively. The boundary between these two segments corresponds to a wide, repeatedly rejuvenated NW–SE transverse dextral fault zone representing the eastern part of the Elbe Fault Zone (EFZ) (Dallmeyer et al., 1995; Edel et al., 2003). In both the southern and northern segments, it is possible to discern autochthonous and the allochthonous domains. The southern part consists of two elongated tectonic windows emerging through high-grade rocks of the Moldanubian (Fritz et al., 1996; Schulmann and Gayer, 2000). The northern, Silesian unit contains Devonian and early Carboniferous mafic volcanic rocks (Dallmeyer et al., 1995). The intensity of the Variscan deformation decreases eastwards; the western part of the Moravo-Silesian zone, close to the boundary with the overriding Moldanubian zone, is composed of a number of allochthonous thrusts sheets, while the east part are mostly in autochthonous position (Dallmeyer et al., 1995; Mazur et al., 2006). The classical tectono-stratigraphic zones of the Variscan orogen have recently been considered to represent separate terranes (e.g., Matte et al., 1990; Franke et al., 2000; Winchester et al., 2002) usually correlated with Armorica and interpreted to form the Armorican Terrane Assemblage (Belka et al., 2000; Tait et al., 2000; Finger et al., 2000; Belka et al., 2002).

The tectonics of the Alpine–Carpathian system was controlled during Tertiary by the N–S convergence of the Adriatic and European plates. The resulting collision caused thrusting and crustal thickening during the continental collision. The Tertiary deformation of the northern Eastern Alps was characterized by northward thrusting and dextral wrenching along WNW-trending strike-slip faults. Presently, in the northern part of the Eastern Alps, the Northern Calcareous Alps, built up by thick Permomesozoic carbonatic layers, are the highest tectonic unit thrust over the Flysch-Helvetic zone and the Molasse zone outcropping in the northern rim of the Eastern Alps. The Molasse zone lies autochthonously on the European foreland in its lower part and partly allochthonously below the Alpine nappes (Reinecker and Lenhardt, 1999).

3. Previous geophysical studies in the area

The attempts to reveal a crustal structure of this region were usually associated with the investigation of the Bohemian Massif (Beránek and Zátopek, 1981) or with the investigation of the Carpathian foreland (Majerová and Novotný, 1986; Bielik et al., 2004). The interpretation of the refraction measurements indicated the pronounced Moho discontinuity at a maximum depth of 39 km in

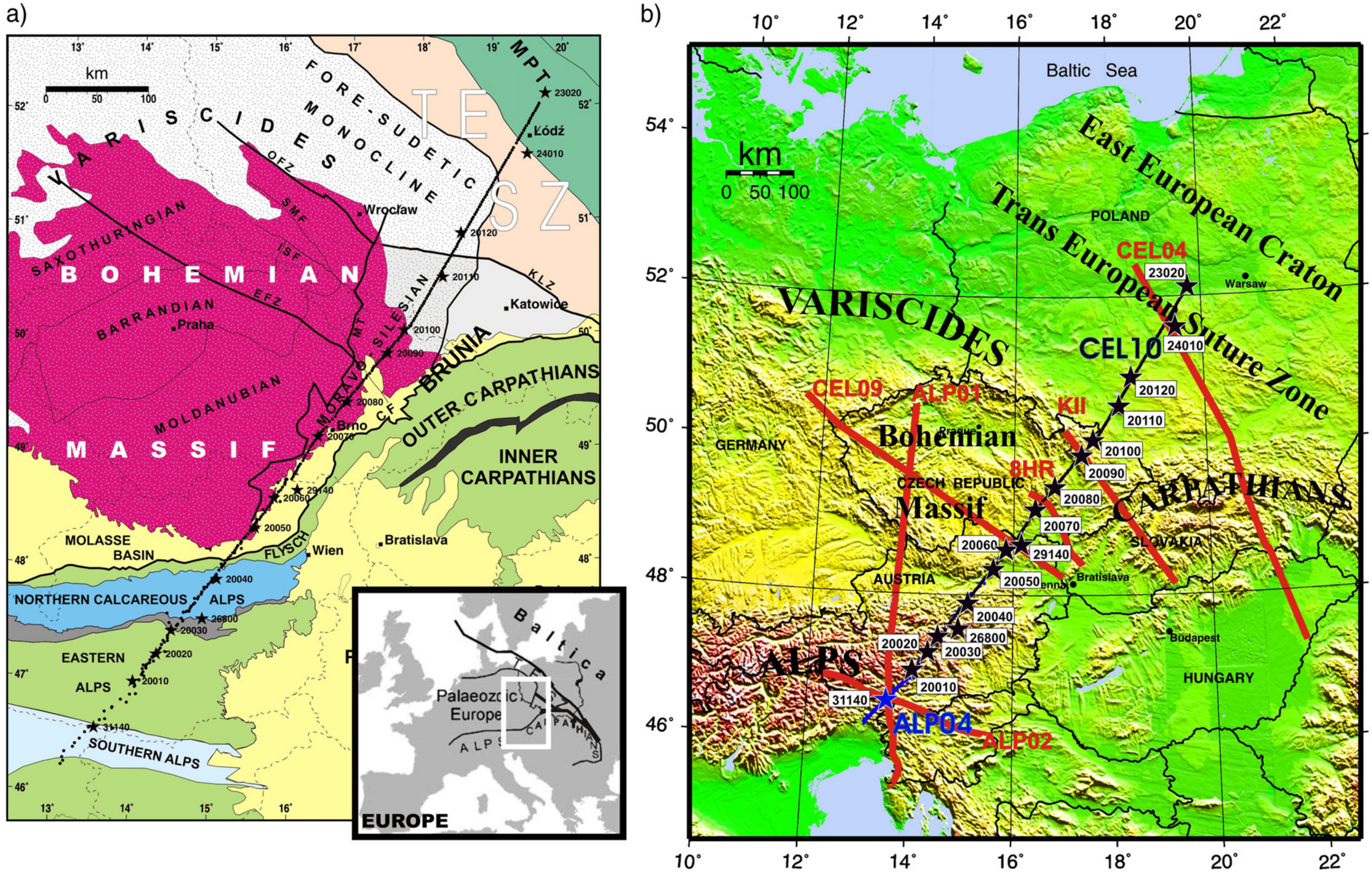

Fig. 1. (a) Location of the profile CEL10 and ALP04 together with the main basement units. The insert shows the study area on a simplified map of Europe. EFZ, Elbe Fault Zone; ISF, Intra-Sudetic Fault; SMF, Sudetic Marginal Fault; OFZ, Odra Fault Zone; KLZ, Kraków-Lubliniec Zone; MT, Moldanubian Thrust; CF, Carpathian Flysch; TESZ, Trans-European Suture Zone; MPT, Mid-Polish Trough. (b) Geographical setting of profile CEL10 and ALP04. Black stars mark positions of individual shot points along the CEL10 profile, blue star refers to the ALP04 shot point. Other seismic refraction and reflection profiles (ALP01, ALP02, CEL09, 8HR, KII, and CEL04) are marked by red solid lines.

the central part of the Bohemian Massif and a less pronounced Moho at a depth of about 32 km at the eastern margin of the Bohemian Massif at its contact with the Carpathians (Beránek and Zounková, 1977). In general, the interpreted profiles were of NW–SE direction, perpendicular to the CEL10 profile. The important contribution to understanding of the geological structure on the contact of the Bohemian Massif and the Carpathians was the interpretation of the regional refraction profile KII extending from the border of the Czech Republic and Poland to Slovakia. In the Silesian zone, the two bands of reflections suggested the Moho located at 36–37 km depth and rising towards the SE to 30–32 km (Majerová and Novotný, 1986). Reflection profile 8HR further to the south (see Fig. 1b), crossing CEL10 at 440 km distance in the Moravian zone, indicated the Moho at 35–37 km depth.

Within the frame of the CELEBRATION 2000 experiment, a refraction and wide-angle reflection profile CEL09, traversing the whole Bohemian Massif, was modelled. Beneath the Moravian unit (360 km along the CEL10 profile), CEL09 data indicate a broad crust–mantle transition zone and suggest a thrusting of the Moldanubian over the Moravian unit in depth (Hrubcová et al., 2005).

The Polish Variscides and the TESZ were broadly investigated during the last 20 years, except for the easternmost termination of the Variscides, corresponding to the location of the NE part of the CEL10 profile. The POLONAISE'97 experiment and earlier deep seismic sounding studies with TTZ and LT profiles provided a good regional picture of crustal structure in western and NW Poland (Guterch et al., 1999; Grad et al., 2003a, 2005). The Variscan crust in this area is 30–35 km thick (e.g., Wilde-Piórko et al., 2005) with a two-layer seismic structure characterized by low P-wave velocities down to the Moho discontinuity (<6.7 km s^{-1}) (Grad et al., 2002; Majdański et al., 2006, 2007) and crustal thickening in the TESZ (Dadlez et al., 2005).

Crustal structure of the Eastern Alps was studied along the N–E oriented TRANSALP profile (Bleibinhaus and Gebrande, 2006) and during the ALP2002 experiment (Brückl et al., 2007), when two crossing profiles ALP01 and ALP02 were interpreted. These investigations reveal deepening of the Moho from the North Calcareous Alps to the south from 38 km to 47 km depth and reflect a crustal thickening during the Alpine orogeny.

4. Data acquisition and processing

The seismic data along two refraction and wide-angle reflection profiles CEL10 and ALP04 were acquired during the international

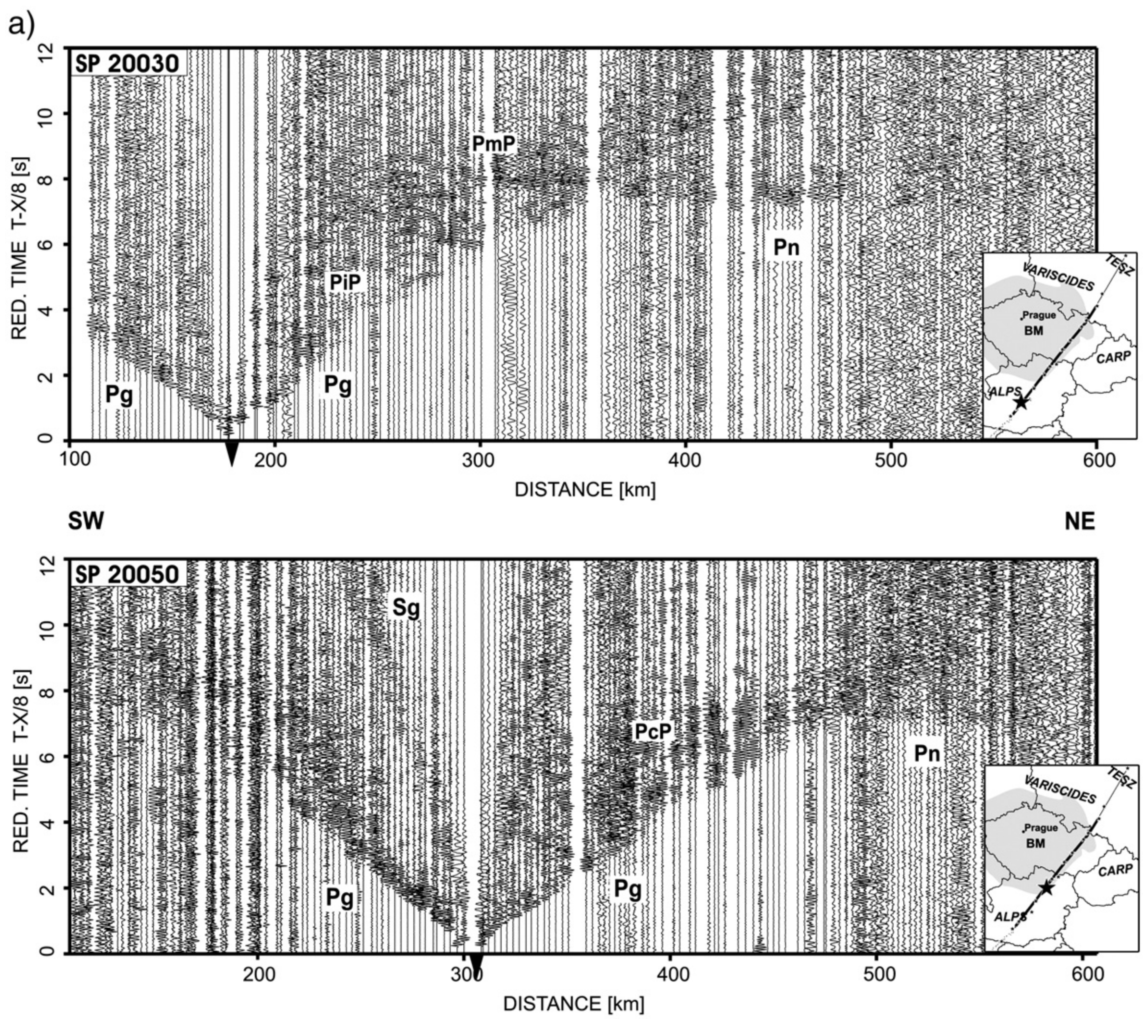

Fig. 2. Examples of amplitude-normalized vertical component seismic sections from different parts along the profile CEL10 plotted with the reduction velocity of 8 km s^{-1} (Fig. 2a–c) and 6 km s^{-1} (Fig. 2d). Identification of main seismic phases: Pg, refraction within the crust; Psed, refraction from the sedimentary cover; Pn, refraction from the uppermost mantle; PmP, reflection from the Moho discontinuity; PcP, reflection from the top of the lower crust; PiP, reflection in the crust. Data have been band-pass filtered from 2–15 Hz. Locations of major tectonic units and shot points are indicated. (a) SP 20030 and 20050 in the SW. Note strong PmP in the Alpine area, vanishing of PmP beneath the Bohemian Massif (SP 20050) and Pn visible to 350 km offset (SP 20030). (b) SP 20080 and 20090 in the Bohemian Massif. Note strong variability of the wave field within individual shot points: SP 20080 — high amplitude Pg phase to the SW, highly reflective crust, and strong decrease of Pg amplitudes to the NE suggesting the existence of very low or negative gradient (LVZ) with corresponding effect on SP 20090. (c) SP 20100 and 20120 in the NE. Note strong PmP with short impulse duration for SP 20120 from the Fore-Sudetic Monocline. (d) SP 24010 and 23020 in the NE with the reduction velocity of 6 km s^{-1}. Note Psed with the apparent velocity of 4.5–5.0 km s^{-1} in the TESZ.

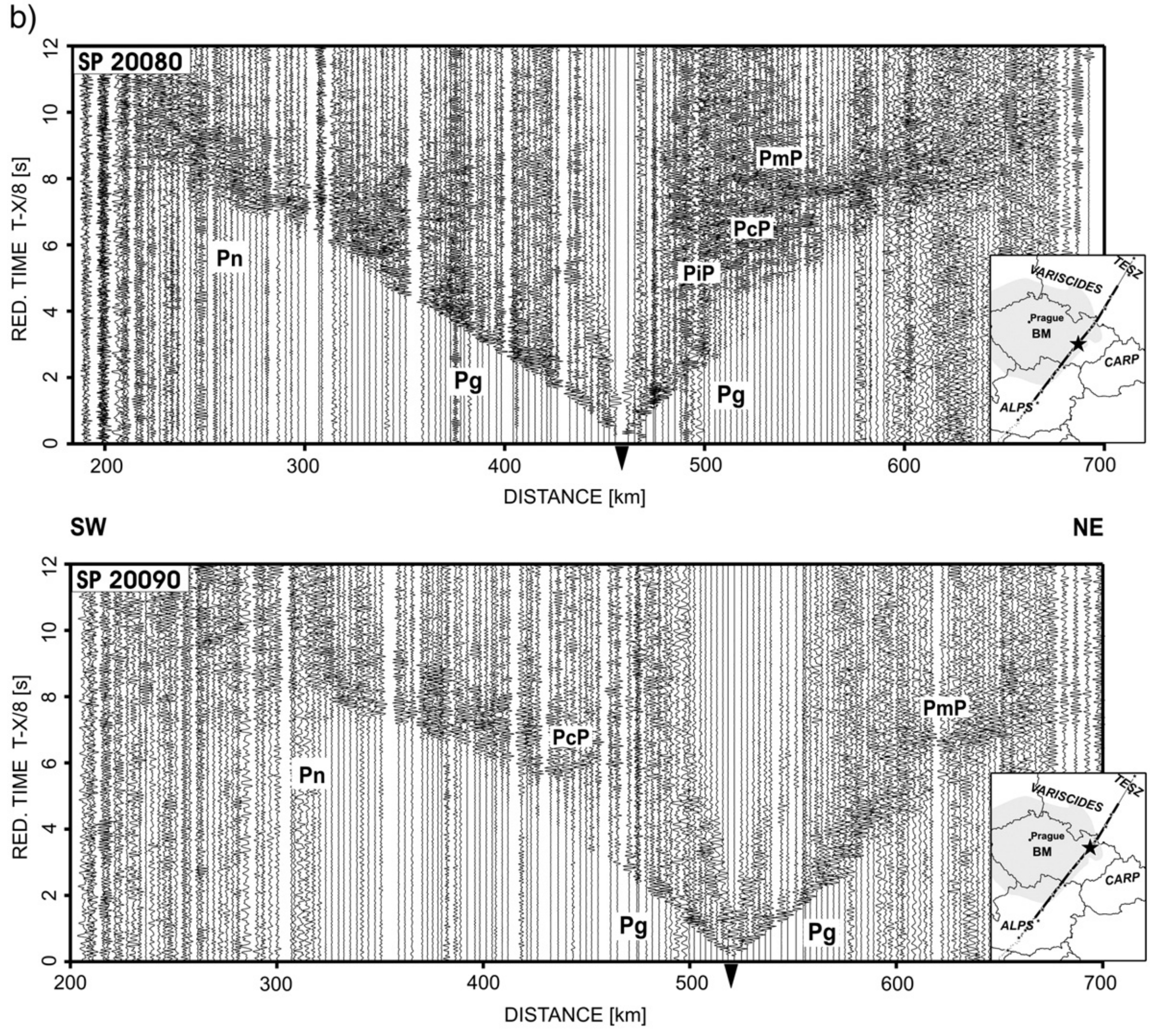

Fig. 2 (*continued*).

seismic experiments CELEBRATION 2000 (Guterch et al., 2003) and ALP 2002 (Brückl et al., 2003). The SW–NE oriented transects CEL10 starts in the Eastern Alps, continues through the Moravo-Silesian zone of the Bohemian Massif, where it strikes the Moravian granitoids and further to the NE the Devonian and Carboniferous Paleozoic cover, continues through the Fore-Sudetic Monocline, and terminates in the TESZ and the Mid- Polish Trough. This profile is 710 km long and comprises 16 shot points. To extend the knowledge of the Eastern Alps and its Variscan basement, profile ALP04 was designed as the extension of CEL10 line to the SW across the Eastern Alps. One shot point was registered along 360 km long profile where 250 km overlapped the CEL10 line (Fig. 1). Thus, the interpreted joint SW–NE oriented profile was 820 km long.

Three shots along CEL10 transects were fired twice or three times and the recordings were stacked in order to improve the signal-to-noise ratio. The average distance between the shots was 30 km with a station spacing of 2.7 km (6 km for ALP04, respectively). The charges amounted to 200 kg on average, for some shot points a charges of 1000–1200 kg were fired. The non-overlapping part of the profile ALP04 comprises 1 shot point with the charge of 300 kg. The positions of shot points and stations were measured by GPS; the origin time was controlled by a DCF77 timer with an accuracy of 3 ms. For more details on geometry of both experiments refer to Málek et al. (2001), Brückl et al. (2003), Guterch et al. (2003), and Růžek et al. (2003). The data from both experiments were sampled at intervals of 10 ms and were recorded mainly by one-component stations REFTEK-125 (TEXAN), complemented by three-component REFTEK and MK-4P stations. The station sensors were 4.5 Hz geophones (1 Hz geophones for three-component stations). Data processing included shot-time corrections and band-pass filtering of the whole data set (usually 2–15 Hz) in order to remove low- and high-frequency noise. The frequency content of the seismic data was highly variable for different shot points, probably due to varying local environment and due to different shooting techniques (borehole shots, quarry blasts). Thus, the filter window was determined interactively during the interpretation, depending on the data quality and the frequency content. Recordings were sorted into shot gathers; seismic sections were trace-normalized to the maximum amplitude along the trace and plotted with a reduction velocity of 8 km s^{-1}.

5. Data description

The seismic data used for the interpretation have good signal-to-noise ratio and allow several P-wave phases to be correlated (see Fig. 2a–d). In the first arrivals, we can distinguish refraction from the upper/middle crust, the Pg phase, and refractions from the upper mantle marked as Pn. Refracted waves from the sedimentary cover (Psed) are observed in the vicinity of shot points in the NE. Clear arrivals of refracted and reflected waves from the crystalline crust and the upper mantle are typically observed up to the offsets of 250–300 km. In later arrivals, we observe the reflections from the Moho discontinuity (PmP) usually as the strongest phase, especially in the

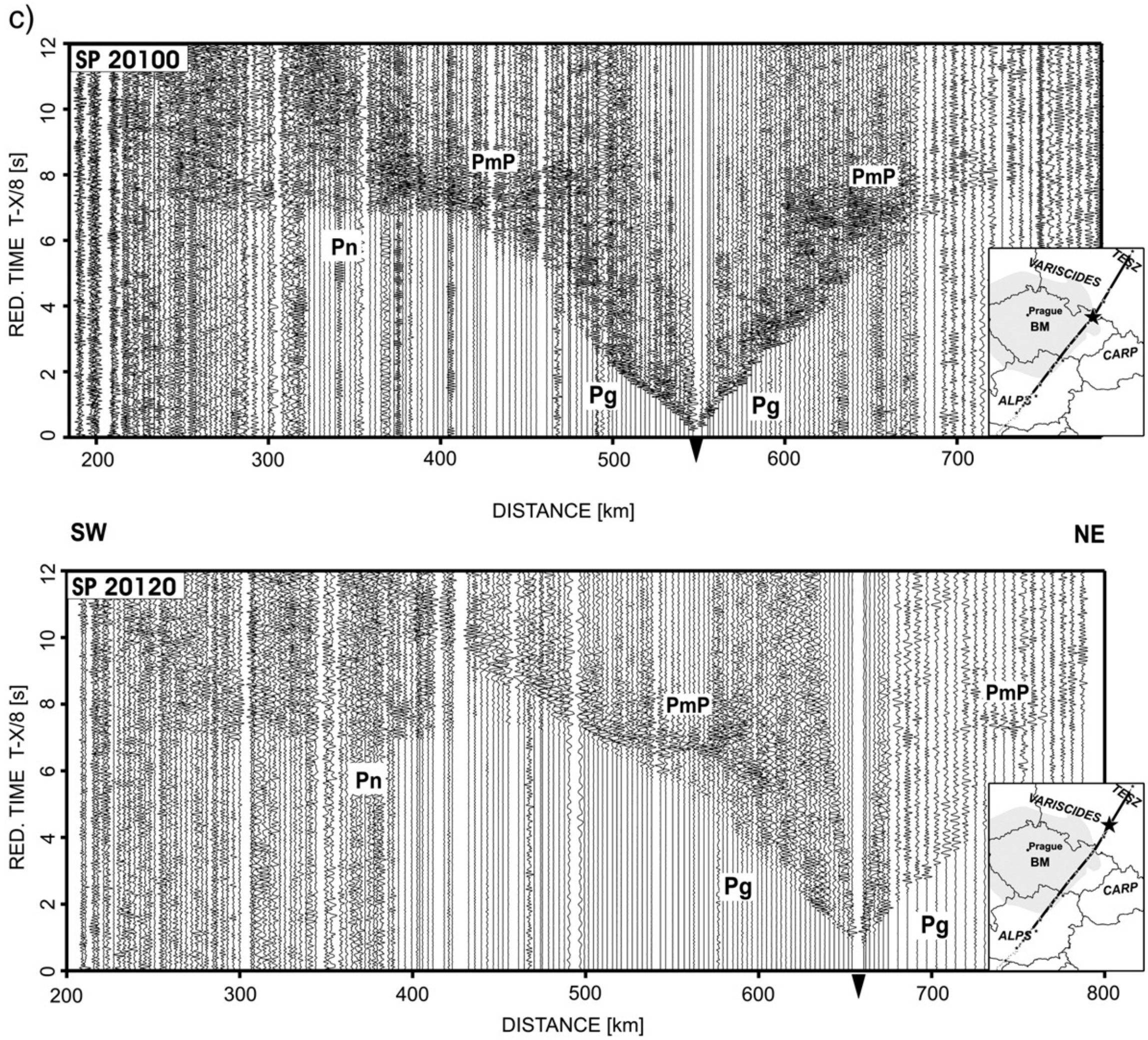

Fig. 2 (*continued*).

NE part of the profile. Reflections from mid-crustal discontinuities are marked as PiP, or PcP for reflections from the top of the lower crust. Fig. 2a–d give the examples of seismic sections in different part along the profile.

5.1. Pg phase

The Pg phase with the apparent velocity of 5.8–6.1 km s^{-1} is usually possible to correlate up to the 100–120 km offsets. The abrupt anomalies of Pg phase reflect the existence of near-surface velocity inhomogeneities. Slightly higher apparent velocities (about 6.2 km s^{-1}) correlate with the mafic volcanic rocks of the Silesian unit at a distance of 510–550 km along the profile.

In the Alpine area (SW part of the profile), SP 20020, 20030, 26800 and reciprocally SP 20050 and 20060 show a jump of 0.35 s on the Pg phase at 235 km along the profile that indicates low velocity zone (LVZ) beneath near-surface rocks at that distance. Moreover, in seismic sections of SP 20020 and 20030 the Pg phase vanishes at about 80 km offsets. The deeper phase P1 has small apparent velocity and thus it cannot be satisfactorily modelled without assuming LVZ at a distance of 180–230 km. The data suggest that the LVZ outcrops at the surface at 250 km distance and dips to the SW (see Figs. 2a, 5). Forward modelling confirmed that hypothesis.

In the middle part of the profile, in the Bohemian Massif, the SP 20080 displays strong differences in the wave field with a high amplitude Pg phase in the SW and a strong decrease of the Pg amplitude with highly reflective middle/lower crust in the NE. The corresponding effect is visible on SP 20090 and 20100 (see Figs. 2b,c, 6) with a Pg amplitude decrease at the offsets between 50–130 km and with a strong intracrustal reflection in later arrivals. It cannot be the effect of trace normalization (a decrease of the Pg amplitudes due to the relatively higher amplitudes of later arrivals, mainly PmP), because amplitude decrease is also observed in the true amplitude scaling. Thus it may suggest the existence of very low or negative gradient zone in the upper crust in that area.

For shot points in the NE (SP 23020, 24010), first arrivals at offsets smaller than 60 and 30 km, respectively show the apparent velocity of 4.5–5 km s^{-1} marked as Psed (see Fig. 2d). This reflects a few to over 10 km thick sedimentary cover in the Fore-Sudetic Monocline and particularly in the TESZ zone.

5.2. Lower crust and mantle phases, PmP reflections

At the lower crustal and uppermost mantle level we can distinguish following differences. While in the Bohemian Massif the crossover distance between the crust and mantle refractions is 160 km and sometimes the Pn is missing, in the SW, in the Alps, the crossover distance is 180 km, indicating a very deep crust. Unfortunately, the most SW section of the profile (SP 31140 from ALP 2002 experiment) enables to correlate the Pg only up to 70 km offset and no Moho

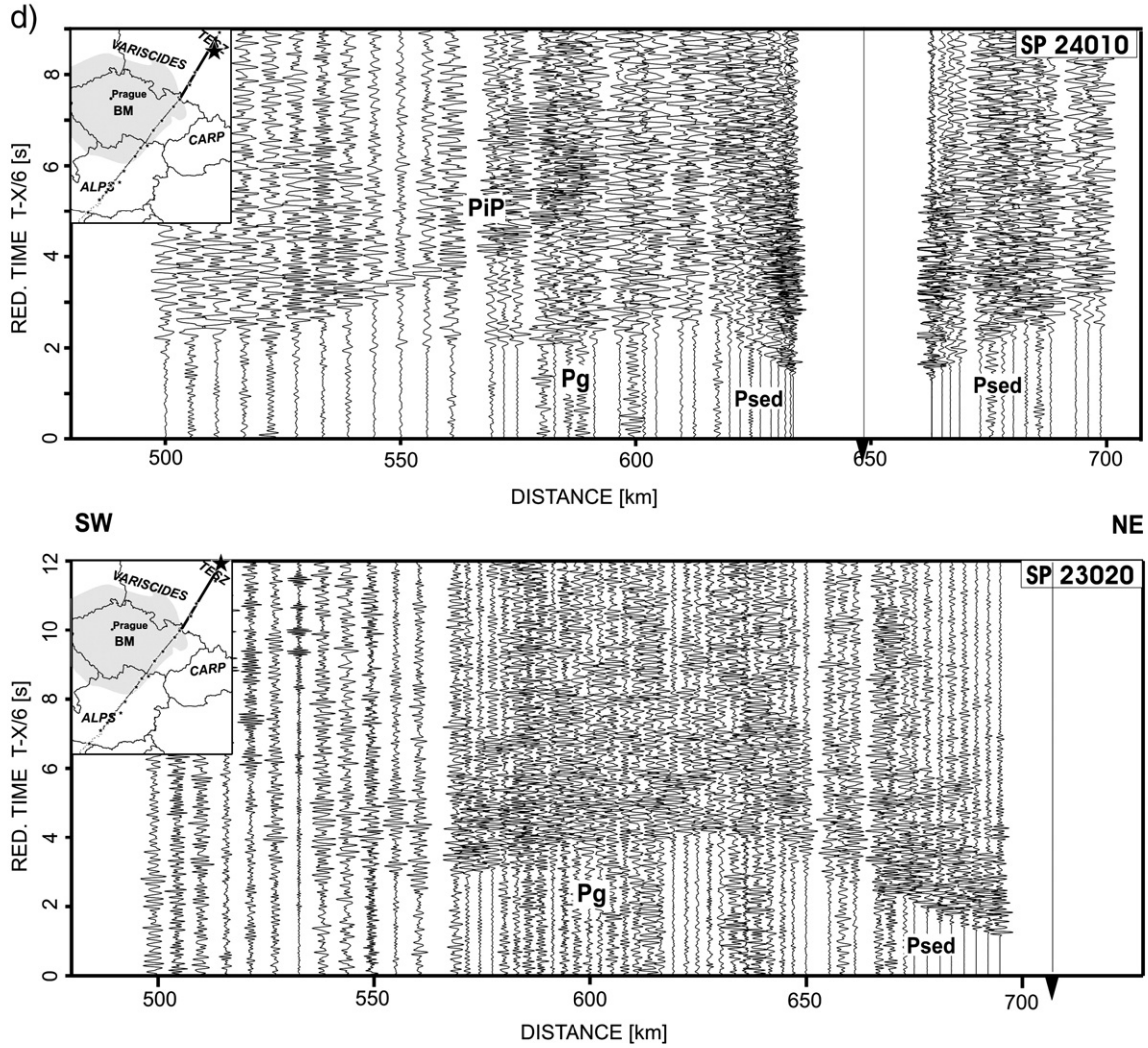

Fig. 2 (*continued*).

reflections are observed, which does not allow for any differentiation of the velocity structure in the deeper crust at the SW termination of the profile.

The Bohemian Massif in the central part of the profile shows strongly reflecting crust with a long coda, while the Moho reflections are not well pronounced (SP 20050, 20060; see Fig. 2a). The local intracrustal reflectors are sometimes hard to correlate in-between shot points. Thus, it is sometimes impossible to perform the reciprocity checking necessary for depth/dip location of the reflectors. Nevertheless, in the middle crust, one consistent reflector is possible to correlate in the SE and central part of the Bohemian Massif. In the NE part of the Bohemian Massif, we can observe a clear PcP phase, interpreted as the reflection from the top of the lower crust (SP20070, 20080 right and SP 20100 left, Figs. 3bc, 6, 7). It is the strongest reflection in these sections and due to its long coda and high amplitude it masks the much weaker PmP reflection.

In the NE, the crossover distance is the shortest and is about 140 km. There, the PmP reflections are the most pronounced compared to other areas along the profile. This suggests a well-defined Moho discontinuity beneath the Fore-Sudetic Monocline and the TESZ, while the weaker PmP phase in the Bohemian Massif indicates the Moho with a relatively low velocity contrast (Figs. 2c, 7).

The Pn phase can be identified as the first arrivals usually at the offsets of 130–230 km, sometimes up to 300 km with an apparent velocity of 8 km s^{-1} on average. It is usually visible in the SW and NE part of the profile, while in the Bohemian Massif it is mostly missing. This enhances the idea of a well-defined Moho in the SW and NE parts of the profile and a less pronounced transition zone in the central part of the profile.

6. P-wave velocity models

6.1. Seismic tomography model

In the first modelling step, we applied the tomographic travel time inversion of the first P-wave arrivals (Hole, 1992) to assess a preliminary 2-D velocity model in the crust. The procedure uses the backprojection algorithm (Humphreys and Clayton, 1988), based on the linearization of the non-linear relation between the travel time and the slowness. The model is defined on an equidistant rectangular grid with the Vp velocities defined at the grid nodes. In the forward step, the travel times are calculated using a finite difference algorithm (Vidale, 1990). In the inverse step, the slowness perturbations are calculated by uniformly distributing the travel time residual along a ray.

For the inversion, the initial 1-D model for the upper crust was calculated by inverting the average Pg travel time curve by the Wiechert–Herglotz formula (Aki and Richards, 1980); for the lower crust and mantle, a smooth arbitrary velocity–depth curve was derived. In total, 1546 first arrival picks from 21 shots were selected

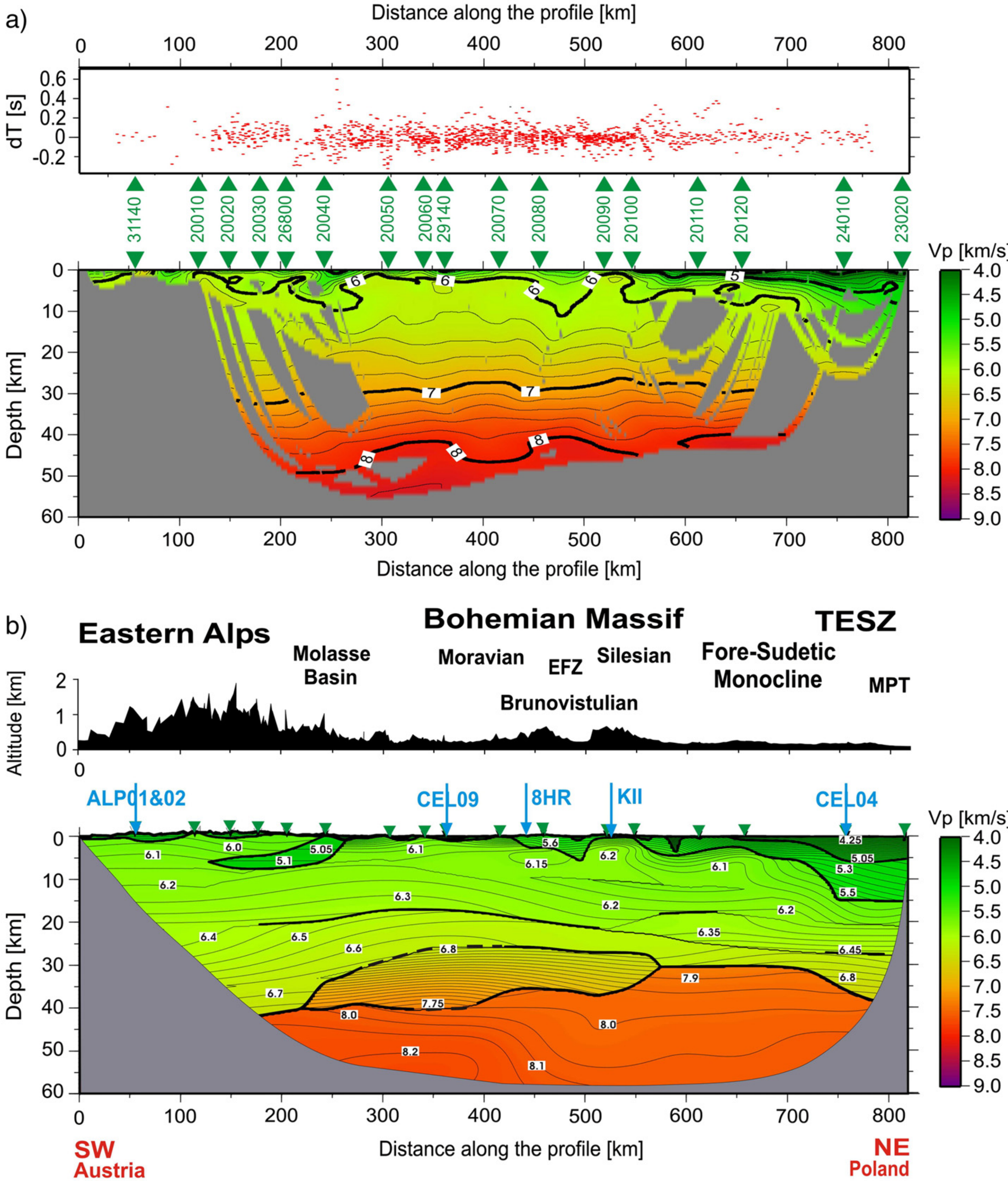

Fig. 3. Two-dimensional P-wave velocity models for the joint profile CEL10 and ALP04. a) Results of 2-D seismic tomography of J. Hole (1992) together with a misfit between the observed and calculated travel times. Numbers represents P-wave velocities in km s^{-1}. b) Results of forward ray-tracing modelling with SEIS83 package (Červený and Pšenčík, 1984) with elevations on the top. The grey covers the unconstrained parts of the model. Thick lines mark discontinuities constrained by the reflections and well-constrained interfaces in the uppermost crust; dashed thick lines mark the layer boundaries where no reflections were observed. Thin lines are the isovelocity contours spaced at the intervals of 0.05 km s^{-1}. Numbered triangles refer to the shot points, arrows show locations of other refraction and reflection profiles. EFZ, Elbe Fault Zone; TESZ, Trans-European Suture Zone; MPT, Mid-Polish Trough. Vertical exaggeration is 1:4.

for the inversion. Picks which could not be reliably identified as first arrivals were not included. The computation was carried out for a model grid size of 1×1 km in 5 subsequent steps, gradually enlarging the data offsets (50, 100, 150, 200 and 400 km) and thus the maximum depth of ray penetration, with several iterations at each step. The smoothing was performed by a moving average filter with cell sizes of 40×10, 20×4 and 10×2. The resolution of the algorithm thus increased gradually and stabilized the inversion. The calculation was controlled by the root-mean-square (RMS) travel time residuals, which amounted to 92 ms for the final model, exceeding approximately twice the level of the estimated picking uncertainty.

The resulting tomographic model and the final travel time residuals are presented in Fig. 3a. The velocity variations in the upper and middle crust indicate differences in the structure of the tectonic

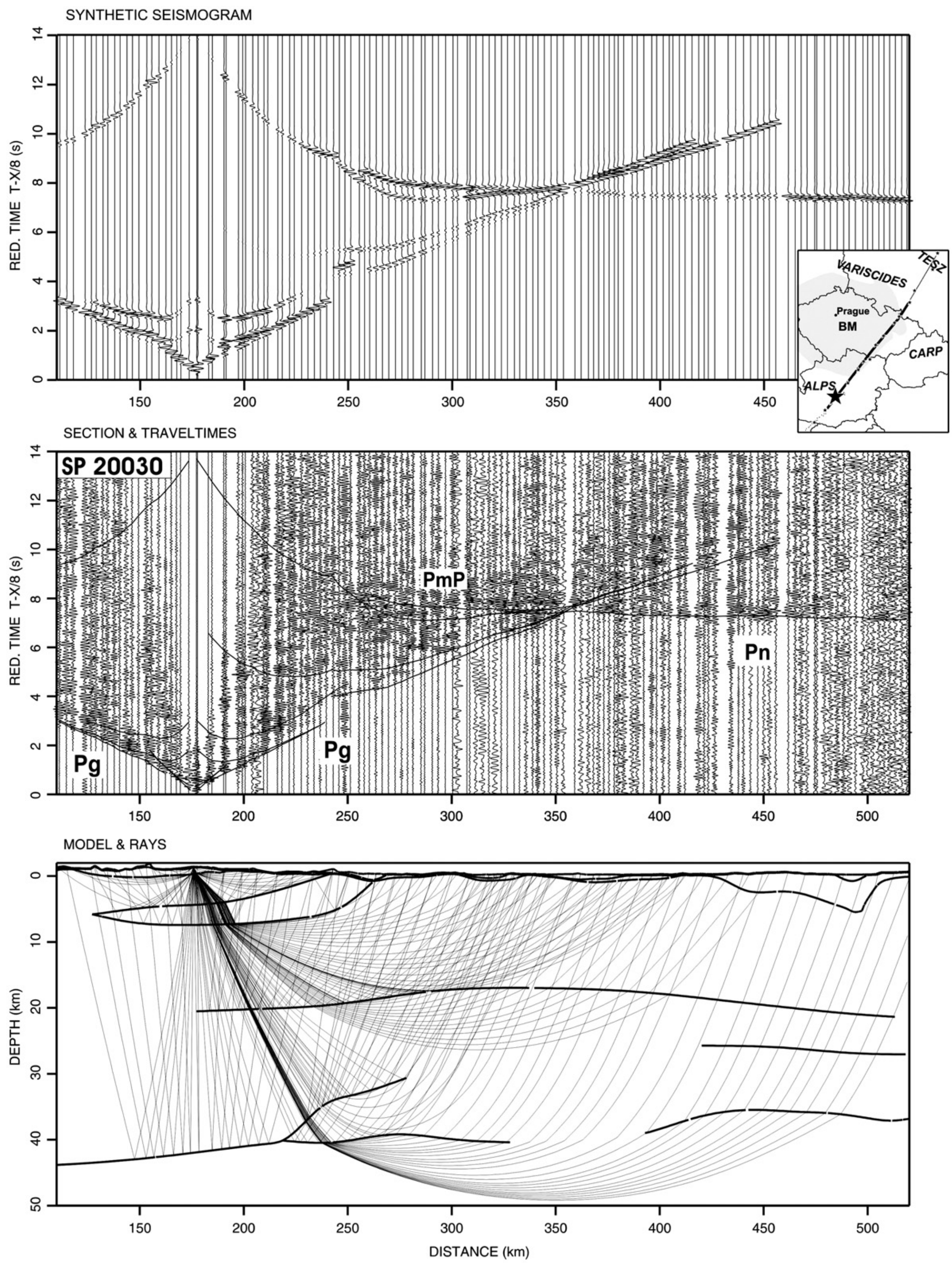

Fig. 4. Example illustrating forward modelling for the SP 20030 from the Eastern Alps area. Top — synthetic section, middle — amplitude-normalized seismic section with calculated travel times, bottom — model and calculated raypaths. Reduction velocity is 8 km s^{-1}, locations of major tectonic units and shot points are indicated. Note strong Pn detected up to 350 km offset in the Bohemian Massif.

units crossed by the profile. The upper crust in the Alpine area at a distance of 150–260 km exhibits the alternations of higher and lower velocities. In the Bohemian Massif, a high near-surface velocity gradient followed by a low gradient in the upper/middle crust is observed. Lower velocities of 5.4–5.8 km s^{-1} down to a depth of 10 km occur near the contact of the Moravian and Silesian units. Considerably lower velocities in the upper crust in the range of 3.0–5.5 km s^{-1} for depths down to 15 km delimit the Mid-Polish Trough of the TESZ in the NE.

In the Bohemian Massif, due to a higher near-surface velocity gradient followed by a low gradient in the middle crust for crystalline rocks, the turning point of the Pg rays is at shallow depths. The rays concentrate in the parts with high velocity gradients and leave the deeper parts of the crust practically unconstrained. For this reason the middle and lower crust with the sparse ray coverage are poorly constrained and lack the velocity differentiation in the tomographic model. Due to the smoothing performed during the inversion and model parameterization, the velocity discontinuities are smoothed into broad gradient zones and the depth of the Moho boundary cannot be reliably estimated from this model.

6.2. Forward modelling results

The smooth tomographic model (Fig. 3a) gives only an approximate distribution of velocities in the crust and mantle and is not sufficient to describe the structure. On the other hand, variations in amplitude, travel time and duration of both the refracted and reflected seismic phases from the crust and uppermost mantle give more constraints on the velocity variations and location of the seismic discontinuities. Modelling of all phase allows for a more detailed velocity image, and for delineation of the reflecting interfaces, including the Moho discontinuity. Thus, we applied the iterative travel time fitting to further refine the tomographic model using the ray-tracing program package SEIS83 (Červený and Pšenčík, 1984) supplemented by interactive graphical interface MODEL (Komminaho, 1997) and ZPLOT (Zelt, 1994). The initial velocity model was based on the final model from the tomographic inversion, and the overall layering was derived mainly according to reflected phases. The modelling also involved the calculation of synthetic sections and qualitative comparison of the amplitudes of synthetic and observed seismograms. Since the amplitudes of seismic waves are very sensitive to the velocity gradients and velocity contrasts at discontinuities, synthetic seismograms were used as an additional constraint. Fig. 4 shows an example of the forward modelling approach for SP 20030 in the Alpine area with calculated travel times and synthetic section, where strong Pn in the Bohemian Massif was detected up to 350 km offset.

The final 2-D velocity model is presented in Fig. 3b. Starting in the SW, in the Alpine area, a higher near-surface velocity of 6 km s^{-1} at 190–220 km distance along the profile corresponds to higher velocities of the Northern Calcareous Alps. They are underlain by a few km thick low velocity zone (LVZ) with the Vp of 5.1 km s^{-1} outcropping at the surface at 250 km distance and dipping to the SW to the maximum depth of 7 km (Fig. 5). It is interpreted as the Molasse and Helvetic Flysch sediments overthrust by the Northern Calcareous Alps extending from 130 to 300 km distance along the profile.

In Fig. 5, two shot points (SP 20030 and 26800) give an example of LVZ modelling below the rocks with higher velocities. It is evidenced by high apparent velocity of the Pg (~6 km s^{-1}) close to the shot points and quick decrease of the Pg amplitude, particularly to the NE. Later arrivals, observed at the offsets beyond 30 km, are delayed by about 2 s with respect to the first arrivals up to 12 km offset generated by the top layer. These delayed arrivals were attributed to the basement, which is separated from the high velocity limestone/dolomite layer by a few km thick low velocity zone. According to the velocity, the low velocity layer can be interpreted as the Molasse and/or Helvetic rocks and/or Flysch underlying the Northern Calcareous Alps with higher velocity values.

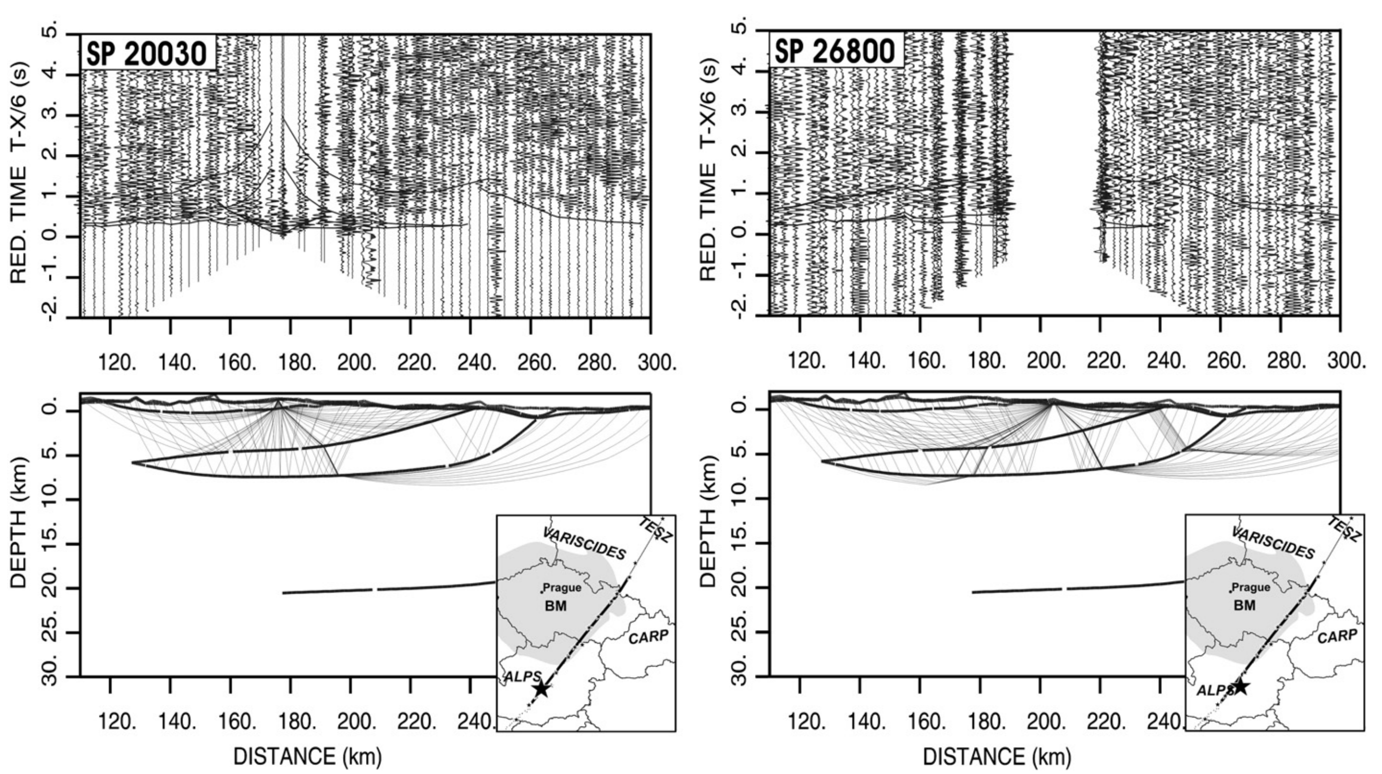

Fig. 5. Examples of forward modelling of the overthrust low velocity zone (LVZ) in the area of the Northern Calcareous Alps. Right – SP 20030, left – SP 26800. Reduction velocity is 6 km s^{-1}, locations of major tectonic units and shot points are indicated. Note high apparent velocity of the Pg (~6 km s^{-1}) close the shot points and fast decrease of Pg amplitude, particularly to the NE.

In the Bohemian Massif, the interpretation along its whole eastern margin is influenced by the fact that this is the area of the Variscan nappes formation, compensated by large faults and shear zones. As such, it represents quite a complicated system and the seismic wave field irregularities reflect the existence of not only velocity inhomogeneities along the profile but also the ones generated by off-line sources. The upper crust of the Bohemian Massif displays a relatively high Vp gradient in the near-surface 2–3 km thick zone with the velocities of 5.8–6.0 km s^{-1} except at its NE end. An almost constant near-surface velocity of 6.0 km s^{-1} is typical especially for the Moravian unit, while the Silesian unit in the NE shows lower Vp velocities with higher gradient. Such feature is characteristic for

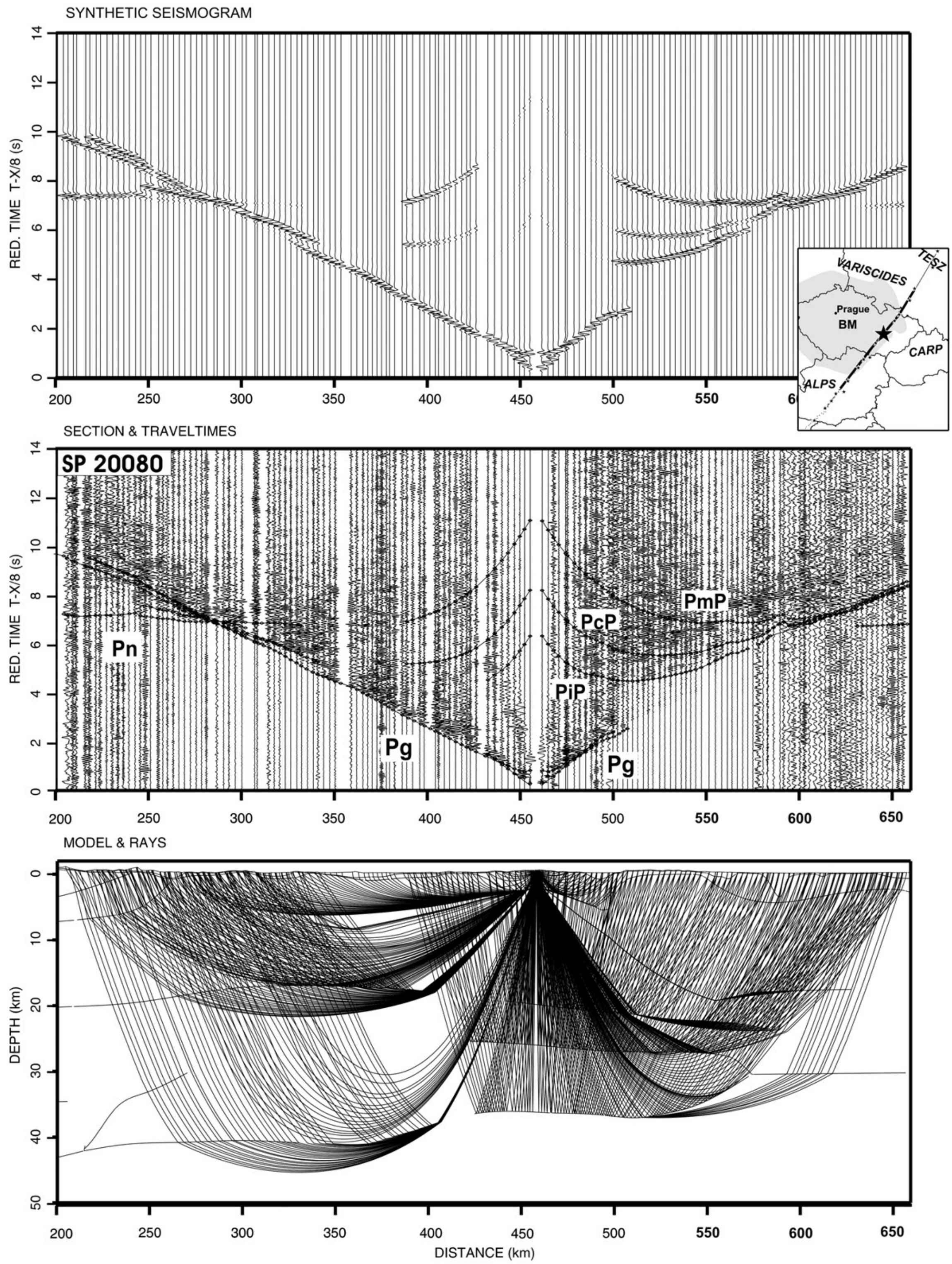

Fig. 6. Example of forward modelling for the SP 20080 illustrating different character of the wave field for two parts of the Bohemian Massif. The SW part shows pronounced, highly reflective Pg phase corresponding to higher velocity gradient (5.8–6.0 km s^{-1}) and no visible reflections from the crust/mantle transition. More to the NE, the fast decrease of Pg wave indicates low gradient. PiP, intracrustal reflection, PcP, reflection from the top of the lower crust. Top — synthetic section, middle — amplitude-normalized seismic section with calculated travel times, bottom — model and calculated raypaths. Reduction velocity is 8 km s^{-1}, locations of major tectonic units and shot points are indicated.

sedimentary rocks and their velocities are in the range from 5.0 to 6.0 km s^{-1} to about 6 km depth. Lower velocities in the range of 5.0–5.6 km s^{-1} down to a depth of 5 km correspond to the Paleozoic sediments on the contact of the Moravian and Silesian units at a distance of 470–510 km along the profile. Very low velocities of 3.9 km s^{-1} to the depth of 0.5 km at the distance of 480 km represent the Neogene sediments of a promontory of the Carpathian foreland. The higher near-surface Vp velocity of 6.2 km s^{-1} at a distance of 510–550 km along the profile coincides with the volcano-sedimentary complex of the Silesian unit (Nízký Jeseník Mts.).

In the NE part of the profile, from 640 km onward, upper crust comprises sediments of the Fore-Sudetic Monocline and the TESZ with velocities in the range of 3.6–5.5 km s^{-1} and maximum depth of about 15 km beneath the Mid-Polish Trough. Significantly lower velocities of 3.7–4.3 km s^{-1} at a distance of 590 km along the profile to a depth of 3 km coincide with the south-eastern extension of the Odra Fault Zone.

In the Bohemian Massif beneath the Paleozoic sediments, the deeper parts of the upper crust are not resolved properly by the tomography and exhibit a very low vertical gradient with the Vp velocity of 6.0–6.1 km s^{-1} from 3 km down to about 10 km depth. Instead of a low gradient, an alternative solution may be to introduce a low velocity layer in the upper crust at a distance of 400–480 km along the profile. However, in our opinion, the data cannot constrain the decrease in the velocity, partly because this area borders with lower velocities (5.0–5.6 km s^{-1}) from the surface down to a depth of 5 km at a distance of 470–510 km along the profile. Therefore we do not describe a LVZ in this part of the Bohemian Massif. In the middle crust, we identified a reflector with a velocity contrast of 0.2 km s^{-1} at a depth range of 17–22 km (PiP phases). It is detectable throughout the whole Bohemian Massif; shallower in the Moravian and dipping in the Silesian units, where it features a higher velocity contrast resulting in the reflected phases with high amplitudes (see Fig. 6).

At the lower crustal/upper mantle depths, the Vp features lateral variations, and the seismic signature of the crust/mantle transition suggests differences in its structure in the Bohemian Massif and its neighbouring units. In the Eastern Alps, the Moho is dipping to the SW reaching the depth of 43–45 km. Similar to the interpretation of profiles ALP01 and ALP02 (Brückl et al., 2007), the lower crustal velocities are within the range of 6.6–6.8 km s^{-1} with a velocity

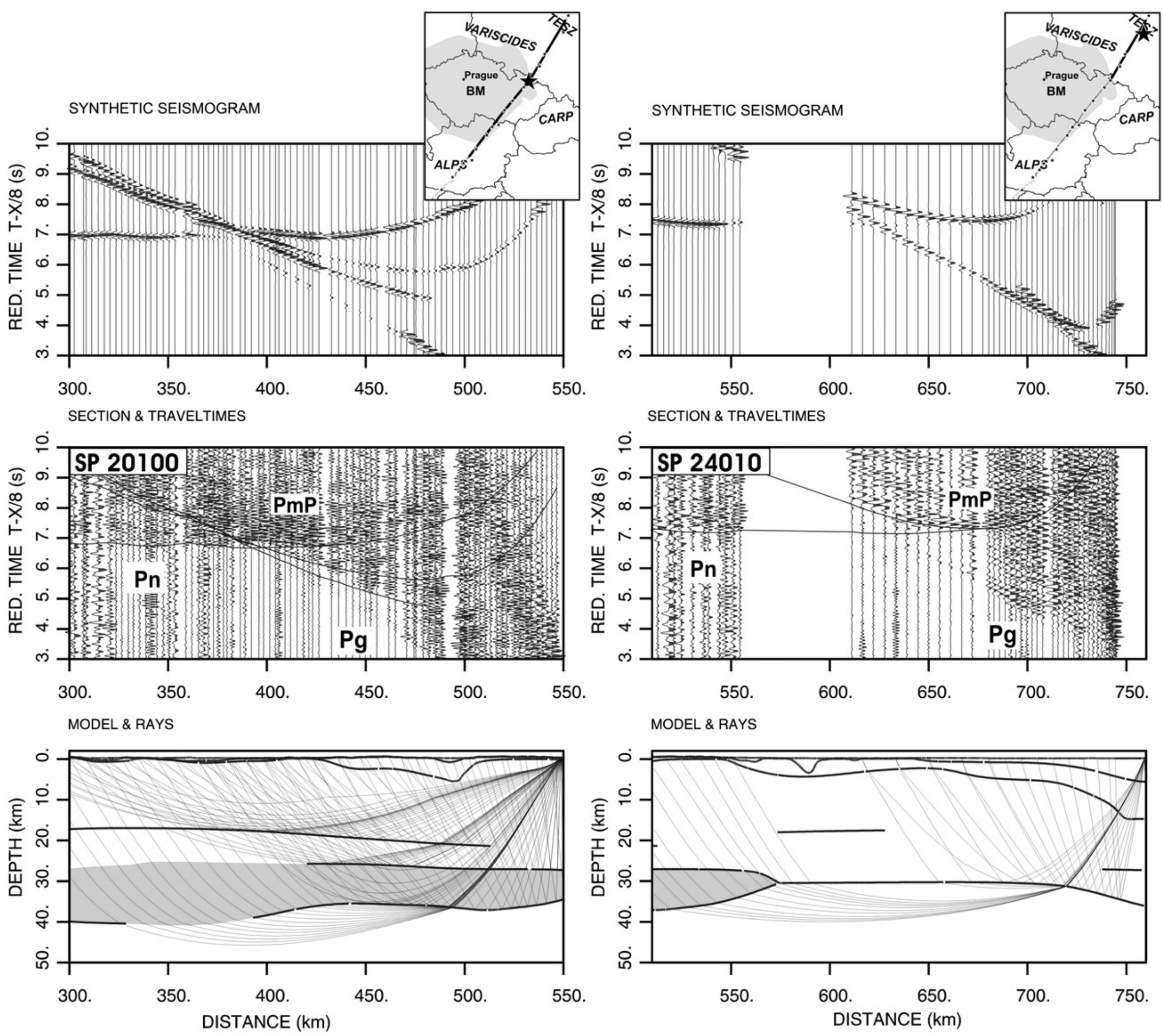

Fig. 7. Examples of forward modelling for SP 20100 and 24010, illustrating the difference in the character of the crust–mantle transition. Note high apparent velocity and long coda of the PmP for the area with high gradient crust–mantle transition zone (SP 20100) and lower apparent velocity and sharp onsets of the PmP for the "normal" Moho discontinuity with high velocity contrast. Top — synthetic sections, middle — amplitude-normalized seismic sections with calculated travel times, bottom — models and calculated raypaths for both shot points. High velocity zone in the Bohemian Massif marked in grey. Reduction velocity is 8 km s^{-1}, locations of major tectonic units and shot points are indicated.

contrast to 8.1 km s^{-1}. The increase in the Moho depth at the distances of 0–220 km along the profile reflects a crustal thickening beneath the Alpine area.

In the deeper parts of the Bohemian Massif's crust, instead of a sharp Moho, we interpreted a lower crustal high velocity layer spreading from 230 to 570 km along the profile. Though, the high velocity lower crustal zone can be viewed as a common feature along the whole eastern margin of the Bohemian Massif, the slightly different character of the wave field suggests differences between the Moravian and Silesian units, crossed by the profile. Beneath the Moravian unit in the SW, a strong lower crustal reflectivity with a long coda and a weak or null PmP phase suggests the existence of a highly reflective zone with high Vp gradient and continuous increase in the Vp from 7.0 to 7.9 km s^{-1} over a depth range of 28–40 km. This gradient zone has no distinct velocity contrast either on the top or in the bottom of this zone. More to the NE, beneath the Silesian unit, the PmP is more pronounced, though it is usually not the strongest reflection. In some sections (SP 20070, 20080, 20090 and 20100, see Figs. 2b,c, 6 and 7), it is masked by stronger reflections at the depths of 26–28 km interpreted as originating at the top of the lower crust. This discontinuity extends from 420 to 570 km distance with a velocity contrast of 0.4 km s^{-1}. Moreover, some sections show a pronounced mid-crustal reflection at 17–21 km depth in this area (Fig. 6). The Moho boundary is modelled with lower velocity contrasts at 35–38 km depth. Velocities in the uppermost mantle are within the range of 7.9–8.1 km s^{-1} with higher values in the SW but they are not well-constrained since the Pn phase is missing in some sections.

Beneath the Fore-Sudetic Monocline, where the PmP phase is the most pronounced in terms of high amplitude and short coda, the Moho is interpreted as a first-order discontinuity at a depth of 30 km with a sharp velocity increase from 6.75 to 7.9–8.0 km s^{-1}. Fig. 7 illustrates the differences in the character of the crust–mantle transition. It compares the PmP with long coda and high apparent velocity originating from high gradient crust–mantle transition zone in the Silesian unit (SP 20100) on one side. On the other side there is the PmP with sharp onsets and lower apparent velocity originating from the "normal" Moho discontinuity with high velocity contrast in the Fore-Sudetic Monocline (SP 24010). Intracrustal interfaces are practically not observed in this area. The Vp velocity in the middle and lower crust increases from 6.6 km s^{-1} at 19–21 km depth to 6.85 km s^{-1} above the Moho, which is in agreement with the velocities along a perpendicular profile (Środa et al., 2006), where the Moho is located at a depth of 35 km with a velocity increase from 6.80 km s^{-1} to 8.15 km^{-1}. The Moho reaches 40 km depth beneath the axial zone of the TESZ, the Mid-Polish Trough (MPT), where the upper mantle velocities are in the range of 7.9–8.1 km s^{-1}.

7. Analysis of accuracy, resolution and uncertainties

Errors of modelling result from combination of several factors: data timing errors, misidentification of seismic phases, travel time picking, inaccuracy of modelling (misfit between data and modelled travel times) and 2-D geometry of the experiment, not accounting for 3-D effects or anisotropy. Some errors are subjective, introduced by

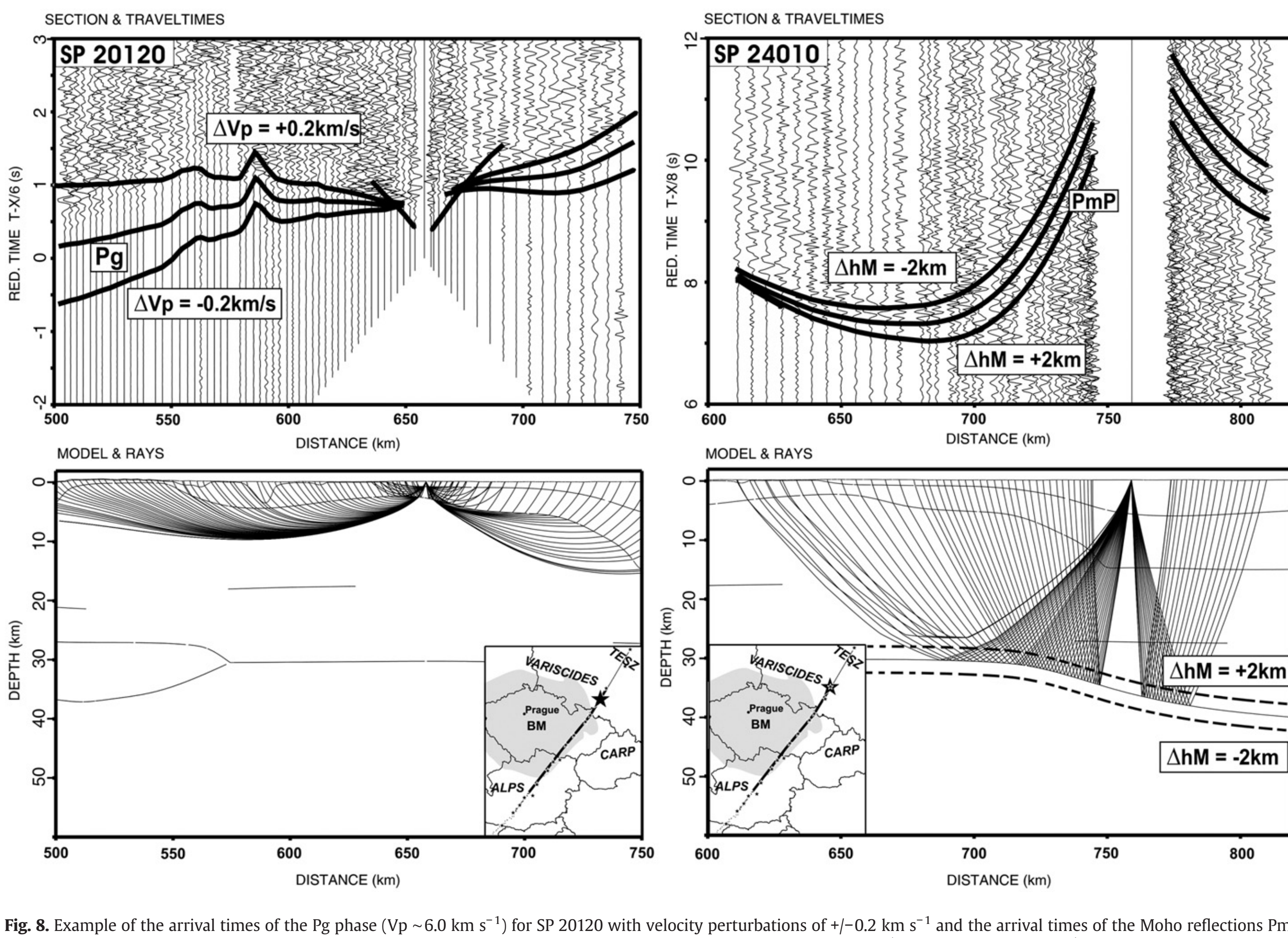

Fig. 8. Example of the arrival times of the Pg phase (Vp ~6.0 km s^{-1}) for SP 20120 with velocity perturbations of +/−0.2 km s^{-1} and the arrival times of the Moho reflections PmP (depth ~30 km) for SP 24010 together with the perturbations of the Moho depth of +/−2 km. Reduction velocity is 6 km s^{-1} (SP 20120), and 8 km s^{-1} (SP 24010). Locations of major tectonic units and shot points are indicated.

the interpreter during phase correlation, and are not possible to quantify. Their magnitude decreases with increasing quality and quantity of data. Due to the subjective errors, it is not possible to produce a full and systematic error analysis. In this study we attempt to evaluate the errors resulting from picking accuracy and from the misfit between the model and the data. Also, in the process of modelling, the limitations of ray theory must be kept in mind. In addition, two-dimensional modelling does not take into account out-of-plane refracted and reflected arrivals, which must have occurred particularly in such a structurally complex area on the contacts of several units.

In the interpreted data set, there were enough data/shots to correlate the major phases with considerable confidence, increased by comparisons of phases picked independently by different interpreters and with the help of reciprocity checking. The calculated travel times fit the observed travel times with accuracy for both refracted and reflected phases of ±0.1 s. The picking accuracy was usually about ±0.05–0.1 s for the Pg phases and about ±0.1–0.2 s for the reflected phases (PmP, mid-crustal reflections) and the Pn. In addition, synthetic seismograms generally showed good qualitative agreement with the relative amplitudes of the observed refracted and reflected phases.

Based on the error analyses for wide-angle data of similar density and quality from the CELEBRATION 2000 experiment (Środa et al., 2006), we assume a standard deviation of the first arrival times to be ~0.1 s or 0.05 s, if we consider near-offset arrivals. For the reflected phases, PmP, which are much harder to correlate, the standard deviation might be as high as 0.2 s. Residuals in the final tomographic models seem to confirm these estimates. In the ray-tracing modelling, we analyze travel time curves rather than single arrivals. In such cases, typical velocity errors, as shown, e.g., by Janik et al. (2002) and Grad et al. (2003a), are in the range of 0.1 km s^{-1} and errors in the boundary depth are of the order of 1 km; however, in complicated parts of the model, they might increase up to 0.2 km s^{-1} and 2 km, respectively. In Fig. 8, we show the arrival times of the Pg phase with the velocity perturbations of +/−0.2 km s^{-1} where the perturbed Pg arrivals are either too late or too early, which illustrates that the velocity in the upper crust can be determined with an accuracy of +/−0.1 km s^{-1}. In a similar way, the arrival times of the Moho reflections PmP are shown together with the perturbations of the Moho depth of +/−2 km.

8. Geological interpretation and discussion

In the following discussion, we propose a general tectonic/geological interpretation for the velocity model along CEL10 and ALP04 profiles at the eastern termination of the Variscan belt. We discuss namely the Moravo-Silesian zone of the Bohemian Massif, and its contact with the Eastern Alps and the TESZ based on the Pg velocity distribution, character of the lower crust and Moho topography, surface geology and results from other profiles, especially ALP01 and ALP02, CEL09, 8HR, and KII.

8.1. Lithology

Interpretation of crustal lithologies along the profile is based on the P-wave velocities obtained by the 2D ray-tracing modelling. The most plausible lithologies are inferred from modelled Vp values compared to global and regional laboratory data for various rock assemblages in the crust (Christensen and Mooney, 1995; Mueller, 1995). Laboratory data are considered at 15 km and 30 km depth, shaded areas represent modelled Vp velocities beneath the interpreted profiles (Fig. 9). In the upper crust, in the Bohemian Massif; the modelled Vp velocities

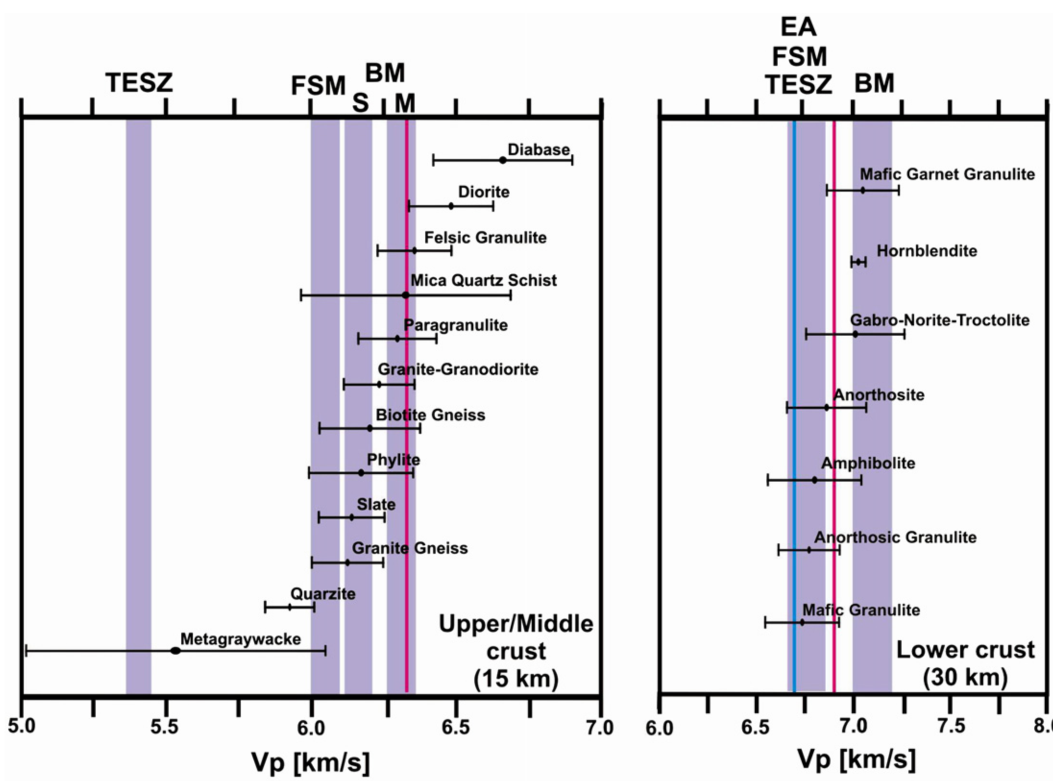

Fig. 9. Comparison of the Vp velocities observed along the joint profile CEL10 and ALP04 with laboratory data according to Christensen and Mooney (1995). Modified after Malinowski et al. (2005). Anisotropy has been neglected. Laboratory data for various rock assemblages in the crust are shown at 15 km (a) and 30 km depth (b). Shaded areas represent modelled Vp velocities beneath the interpreted profiles, and in the upper/middle crust they are 6.3 km s^{-1} for the Moravian (M) and 6.15 km s^{-1} for the Silesian (S) (both the Bohemian Massif BM); 6.05 km s^{-1} for the Fore-Sudetic Monocline (FSM); 5.4 km s^{-1} for the TESZ. In the lower crust they are 7.2 km s^{-1} for the BM and 6.75 km s^{-1} for the Alps, FSM and TESZ. The shaded areas are shown with the estimated uncertainty of the velocity values of ±0.05 km s^{-1} for the upper/middle crust and ±0.1 km s^{-1} for the lower crust. Vertical lines represent calculated velocities for the extended crust — BM (6.31±0.32 km s^{-1} for 15 km depth, 6.89±0.40 km s^{-1} for 30 km depth) (Christensen and Mooney, 1995).

are 6.3 km s^{-1} for the Moravian and 6.15 km s^{-1} for the Silesian; 6.05 km s^{-1} for the Fore-Sudetic Monocline; and 5.4 km s^{-1} for the TESZ. In the lower crust they reach 7.2 km s^{-1} for the Bohemian Massif and 6.75 km s^{-1} for the Alps, the Fore-Sudetic Monocline and the TESZ. The shaded areas are shown with the estimated uncertainly of the velocity values of ±0.05 km s^{-1} for the middle crust and ±0.1 km s^{-1} for the lower crust. Bars represent published standard deviations for laboratory data. Anisotropy has not been taken into account, however it might reach values from 1–5% (e.g. igneous rocks, gneiss, quartzite, granulites, eclogite), to even 10–20% (e.g. phylite, mica schist, amphibolite) (Christensen and Mooney, 1995).

The upper crust in the Bohemian Massif shows velocities typical for granitoids and gneisses, which corresponds to the abundance of plutonic basement rocks of Cadomian age in the Moravo- Silesian unit. Although they occur directly at the surface only in a minor part in tectonic windows, they are known from drillings and geophysical research to occupy at least one third of the entire basement (Dallmeyer et al., 1995). Cadomian plutons are bodies of granitoid gneisses with more granitic composition in the S, while to the N they change to the rocks of intermediate to basic composition as e.g. the intrusions of diorites exposed at the surface at around 420 km along the profile. The velocities in the Silesian unit at the upper/middle crustal level are comparable to that of the Moravian unit which points to a similar origin. Uppermost crustal velocities of about 5.5 km s^{-1} represent the Culm sediments. The velocity model evidences higher velocities of 6.2 km s^{-1} in the upper crust at around 530–540 km along the profile, which can be attributed to basalts of neo-volcanics, though their occurrence is much more limited to a smaller area. The anomalous low velocity upper crust of the TESZ can be interpreted as an extensive pile of sediments and low-grade metasediments (e.g. metapellites, metagraywacke) (Grad et al., 2002, in press). Modelled lower crustal Vp velocities for the Alps, FSM and TESZ are 6.7–6.8 km s^{-1}, which may correspond with gabbros and granulites. On the other hand, for the Moravian and Silesian, the Vp in the lower crust is in the range of 6.8–7.8 km s^{-1}, which can be explained by the presence of mafic garnet granulite, assuming that its content in the lower crust increases with depth as a result of phase transition of rocks with gabbroic composition. Large differences in lower crustal velocities between the Bohemian Massif and the surrounding areas with possibly similar composition may have resulted from a different tectonic evolution and different *P*–*T* conditions.

Christensen and Mooney (1995) divided the crust into five tectonic provinces, where central Europe belongs to the extended crust. If we compare their weighted calculated velocities for the extended crust (6.31±0.32 km s^{-1} for 15 km depth, 6.89±0.40 km s^{-1} for 30 km depth; vertical lines in Fig. 9), the modelled lower crustal velocities in the Bohemian Massif are slightly higher (7.1 km s^{-1}).

8.2. Eastern Alps

During the formation of the Eastern Alps, northward thrusting of nappes occurred along the northern rim of the orogen. Thus, the alternation of higher and lower velocities dipping SW in the upper crust is interpreted as the Molasse and Helvetic Flysch sediments beneath the Northern Calcareous Alps (LVZ at 130–260 km distance along the profile). The interpreted result corresponds with Giese and Prodehl (1976), where they describe an overthrusting of Permomesozoic Northern Calcareous Alps over the Flysch-Helvetic and Molasse outcropping in the northern rim of the Eastern Alps. According to e.g. Reinecker and Lenhardt (1999), the Molasse is detectable not only on the surface but lies allochthonously below the Alpine nappes and its lower velocities alternate with higher velocities of the thick carbonate layers of the Northern Calcareous Alps (Figs. 3, 12). It also corresponds with the results of Behm et al. (2007), where lower velocities of the Molasse Flysch shift in the southern direction with the increasing depth.

We interpreted the base of the Northern Calcareous Alps at 2–5 km depth with the SW dip and Vp of 5.9–6.1 km s^{-1}. The thickness of limestones and dolomites in the Northern Calcareous Alps was interpreted by Giese and Prodehl (1976) and resulted in about 3 km with the P-wave velocities from 5.5 km s^{-1} at the surface to more than 6.5 km s^{-1} at the base. The difference in the velocity compared to our results might be explained by the fact that Giese and Prodehl's results concern the area located about 100 km to the west from the CEL10 profile.

Beneath the Flysch/Molasse low velocity layer, velocities of 6.2 km s^{-1} represent Palaeozoic rocks of the Bohemian Massif, overthrust by the Alpine units and forming their basement. From our data, it was not possible to determine how far to the south the Bohemian basement continues beneath the Alps, but it probably underlies at least the whole lower velocity layer, which extends to the south to a distance of 150 km along the profile.

Beneath the Eastern Alps, the crust thickens and the south-westward dip of the Moho continues to reach the maximum thickness of 40–44 km closer to the axis of the Eastern Alps. The velocity contrast at the Moho is from 6.7 km s^{-1} in the lower crust to 8.2 km s^{-1} in the upper mantle. This interpretation correlates with the results of the interpretation along the ALP01 and ALP02 profiles from ALP 2002 experiment (Brückl et al., 2007), which interpreted the Moho at 43 km and a velocity contrast from 6.6 km s^{-1} to 8.2 / 8.0 km s^{-1}, respectively. Behm et al. (2007) in determination of the Moho show a deeper Moho at the Alpine root compared to a shallower Moho in the Bohemian Massif. Such results reflect the thickening of the crust in a consequence of large-scale collision of the Adriatic and European plates during the Tertiary.

8.3. Bohemian Massif

8.3.1. Upper crust of the Bohemian Massif

The Moravian unit in the SW consists of the metamorphic rocks intruded by Cadomian granitoids and is characterized by a velocity of 5.9–6.0 km s^{-1} down to a depth of 2–3 km. This velocity gradient in the crystalline rocks is usually due to the closing of micro-cracks under increasing pressure. The Cadomian granitoids of the Brunovistulian block in deeper parts of the upper crust show very small, sometimes even negative, vertical gradients as indicated by fast decay of the Pg phase amplitude.

More to the NE, in the Silesian unit, the high velocity gradient in the upper crust is related to the sedimentary rocks of Devonian and Carboniferous deposits covering the Brunovistulian foreland. Higher near-surface velocities at a distance of 500–550 km along the profile can be explained by the occurrence of the Devonian and early Carboniferous mafic volcanic intrusions (Dallmeyer et al., 1995), which increase the average Vp of the sedimentary layer to 6.2 km s^{-1}. A major concentration of volcanic bodies exposed on the surface lies in the vicinity of Bruntál in the Nízký Jeseník Mts. (535 km along the profile) and they are documented also in mines and by geophysical investigations (Gruntorád and Lhotská, 1973). Also, this area coincides with the location of the Quaternary volcanoes.

Lower velocities in the range of 5.0–5.6 km s^{-1} down to a depth of 5 km at a distance of 465–500 km along the profile might represent the SE extension of the Elbe Fault Zone (EFZ) (e.g., Mazur et al., 2006), the crustal scale NW–SE trending zone separating the northerly Sudetic realm from the main part of the Bohemian Massif (e.g. Schulmann et al., 2005) and limiting the contact of the Moravian and Silesian units (Dallmeyer et al., 1995). It is also the area of the increased tectonic activity manifested by the increased seismicity in the eastern part of the Bohemian Massif. Špaček et al. (2006) showed that the majority of seismic activity of swarm-like sequences is concentrated in a 40–60 km wide zone of generally NW–SE trend, crossing the profile in the 465–500 km distance range, which represents a regional zone of weakness. These authors also attribute this zone to the continuation of the Elbe Fault Zone (EFZ), where the increased tectonic activity can be interpreted as a result of the abundance of faults and their interconnection into major fault systems, together with the neo-volcanic activity in the Nízký Jeseník Mts. in the vicinity.

The northern termination of the Bohemian Massif is often thought to be docked by the Odra Fault Zone, a few-km-wide vertical zone liable to the interpretation as a major wrench compatible with the EFZ (Elbe Fault Zone) (Dallmeyer et al., 1995). Low upper crustal velocities of 3.5 km s^{-1} at a distance of 590 km along the profile may represent the south-eastern extension of this Odra Fault Zone and the extension of the Variscan basement exposed at the surface.

8.3.2. Lower crust of the Bohemian Massif

Along the whole eastern margin of the Bohemian Massif, the lower crust is characterized by elevated the velocities of 6.8 to 7.8 km s^{-1}; however, its properties differ between the Moravian and Silesian units along the profile. At the base of the crust in the Moravian area, we do not observe a regular Moho discontinuity with a velocity contrast. The lower crustal arrivals with a long coda and a weak PmP phase with high apparent velocity suggest a high gradient (6.9–7.9 km s^{-1}) reflective layer extending from the middle crust to the mantle, in the depth range of 26–40 km. This layer represents a broad crust–mantle transition zone spreading in the range of 230–400 km along the profile, with no distinct velocity contrast either on the top or bottom. Such a result is consistent with the interpretation of the SE part of CEL09 profile from the CELEBRATION 2000 experiment, where no Moho is imaged as a first-order discontinuity. Hrubcová et al. (2005) interpreted the Moho along the perpendicular CEL09 profile as a broad crust/mantle transition zone with the velocities increasing gradually from 6.8 to 7.8 km s^{-1} over a depth range of 23–40 km (Fig. 10).

More to the NE beneath the Silesian unit, a strong reflector at the depths of 26–28 km represents the top of the lower crust extending from 420 to 560 km along the profile with the velocity contrast of 0.4 km s^{-1} (SP 20080, 20090 and 20100, Figs. 2b,c 6, 7). This reflector is the highest amplitude event within the crust in this area and, together with the poorly pronounced Moho at 35–38 km depth, delimits the lower crustal layer. These results support the interpretations along two perpendicular lines, the reflection profile 8HR and the refraction profile KII. The reflection profile 8HR, which crosses the CEL10 transect in the Brno massif at a distance of 440 km, showed the Moho at 35–37 km (Hubatka and Švancara, 2002a). The KII profile, which crosses the CEL10 transect at 530 km distance, images a strong reflector in the lower crust (28–30 km depth) dipping towards the SE and two bands of reflections at a depth of 36 and 37 km, rising towards the SE to 30–32 km (Majerová and Novotný, 1986; Hubatka and Švancara, 2002b). A

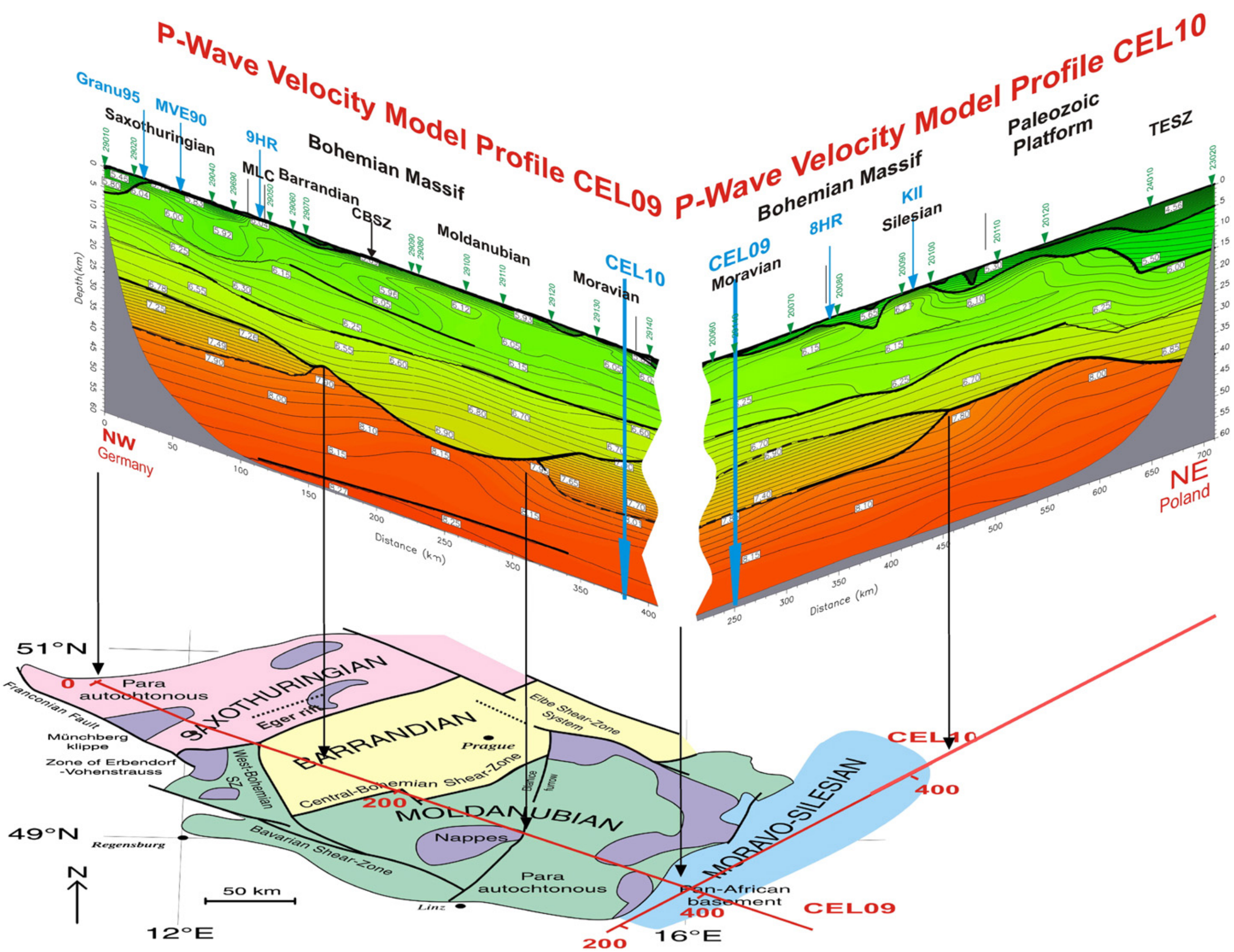

Fig. 10. P-wave velocity models along the profiles CEL10 and CEL09 (Hrubcová et al., 2005) at the crossing point of both profiles, superimposed on a schematic map of major tectonic units of the Bohemain Massif. In the Moravian, the Moho is viewed as a broad crust/mantle transition zone with velocities increasing gradually from 6.8 to 7.8 km s^{-1} over a depth range of 23–40 km.

similar lower crustal layer with the same velocity (in the range of 7.1–7.2 km s^{-1}) was also interpreted by Malinowski et al. (2005) for the Upper Silesian Block, about 100 km to the east. Though their results of the interpretation (along CEL02 profile) differ in having much thicker middle crust (velocities of 6.5 km s^{-1}) compared to the results in our part of the Silesian unit (velocities of 6.2 km s^{-1}), both profiles show similar lower crust with high P-wave velocities.

The origin of the high gradient reflective lower crustal zone might represent gradual changes of the lower crustal composition, with the percentage of mafic/ultramafic material increasing with depth. Alternative explanation may involve a change in metamorphic grade with an incomplete phase transition of granulitic rocks from amphibolite to eclogite facies (e.g. Thybo et al., 2003), where velocities can range from 7.0 to 7.7 km s^{-1} depending on the metamorphic grade, composition and *P–T* conditions (Furlong and Fountain, 1986; Hurich et al., 2001). Such metamorphic processes are commonly associated with lithospheric plate boundaries, where the interactions between plates can produce sufficient heat for metamorphism of the crustal rocks on a large-scale. The lower crustal zone might be also affected by solidified intrusions most probably of amphibole rich composition, which is commonly considered as the magmatic underplating (e.g., Furlong and Fountain, 1986), where seismic velocities might be in the range from values intermediate between crustal and mantle values (7.1–7.5 km s^{-1}) to values typically interpreted to represent mantle material with velocities greater than 7.8 km s^{-1} (Furlong and Fountain, 1986). Magmatic underplating can be attributed to subhorizontal laminae of the dense mafic rocks or melt within felsic granulites (Handy and Streit, 1999), or represented by garnet pyroxene granulites (Morozov et al., 2001).

Schulmann et al. (2008) suggest that the orogenic lower crust in the Bohemian Massif represents Neoproterozoic-Cambrio-Ordovician continental crust that experienced a major thermal reworking during the Devonian where also mantle was involved during Carboniferous. This led to continuous convergent motion of the Brunia continent towards velocities of Moldanubian and a major shortening with extrusion of the granulized lower crust to higher crustal levels. Thus the metamorphic change with possible perturbations of the granulized lower crust is the most probable cause of the high gradient reflective lower crust.

The structural complexity of the Bohemian Massif and adjacent areas led some authors to propose a small-scale mosaic of microplates (e.g. Oliver et al., 1993) but the detailed evaluation of the new findings showed that the north and east parts of the Bohemian Massif are attributed to one Variscan orogenic cycle. Variscan convergence resulted in the Devonian subduction and the early Carboniferous collision. Tectonic structure reveals an overthrusting directed to the NE at the southern flank of the Variscides. The crystalline basement of the whole area is composed of the Brunovistulian and the Moravo-Silesian zone can be seen as a zone of deformation along the Moldanubian Thrust where the Brunovistulian rocks emerge through it in some tectonic windows (e.g., Schulmann et al., 2005, 2008). From this point of view, it is not possible to discern the contact of the Moravian and Silesian units in the depth and the difference can be seen only on the surface, where the area east of the Moldanubian Thrust is covered by clastic sediments of the Culm.

The differences in the character of the lower crust and the Moho between the Moravian and Silesian units might be attributed to the differences in a distance of the profile from the Moldanubian Thrust front, which is oblique to the CEL10 transect. The studied part of the Moravian unit in the SW is located close to this major contact thrust zone. Strong metamorphism and tectonic deformations at this contact zone might contribute to transformation of the original lower crustal architecture into a high Vp and high gradient layer. The Silesian part of the profile in the NE is more distant from the Moldanubian Thrust front and might be less affected by the tectonic processes, which resulted in retaining a more typical character at the lower crust and Moho level with more pronounced velocity discontinuities. Schulmann et al. (2005) show a different type of contact of the Brunia promontory in the southern and northern parts of the Bohemian Massif. As discussed above, the contact with the Moldanubian resulted in the underthrusting of the Brunia promontory beneath the Moldanubian. In contrast, the Brunia continent was not underthrust beneath the orogenic root in the northern sector which might contribute to different character of the lower crust beneath Silesian.

Schulmann et al. (2008) in discussing the characteristics of the lower crust at the eastern sector of the Variscan orogenic belt suggest vertical exhumation of a deep orogenic lower crust followed by subhorizontal escape. They conclude that this early exhumation was kinematically related to the Saxothuringian continental subduction to the east, creating a convergent accretionary wedge west of the Silesian. Fig. 11 shows the comparison of 1-D velocity models for the Silesian and the Saxothuringian crusts. The 1-D velocity characteristics for the Silesian unit was taken from the profile CEL10 at 465 km distance, 1-D velocity characteristics for the Saxothuringian unit was derived from the profile CEL09 at 105 km distance in the west part of the Bohemian Massif (according to the interpretation of Hrubcová et al., 2005). The similarities of the Vp velocities for both these regions can suggest that the Silesian crust is roughly similar to that of the Saxothuringian, especially in its lower parts. This might show some affinity of the Silesian and the Saxothuringian zone as proposed also by e.g. Edel et al. (2003) though more detailed analysis is beyond the scope of this study.

Franke and Żelaźniewicz (2002) and also Mazur et al. (2006) mention the record of the Moravo-Silesian belt that has much in common with that of the Rhenohercynian Belt: Devonian rifting and mafic volcanism, Middle and Late Devonian Reef carbonates, as well as Early and Late Carboniferous deposits. They discuss that the high pressure rocks contained in the structurally highest unit of Jeseniky segment represent deeper parts of the Rhenohercynian / Moravo-

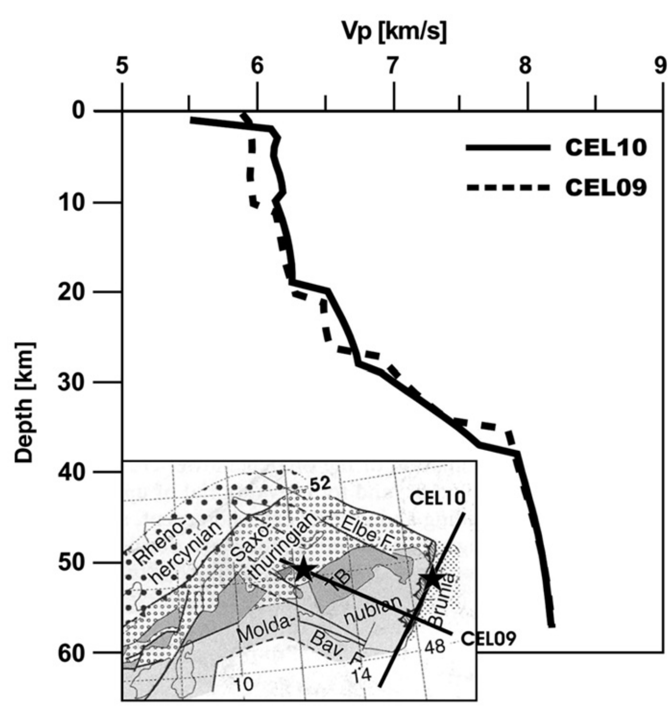

Fig. 11. Comparison of a velocity/depth curve for the Silesian and Saxothuringian units. Solid line: 1-D velocity characteristic for the Silesian taken from the profile CEL10 at a distance of 465 km. Dashed line: 1-D velocity characteristic for the Saxothuringian taken from the profile CEL09 at a distance of 105 km in the west part of the Bohemian Massif (according to the interpretation of Hrubcová et al., 2005). Note similarities of Vp velocities for both these regions especially in their lower parts. The insert modified after Schulmann et al. (2008), stars represent locations of 1-D models.

Silesian basin, which were subducted, then exhumed and overthrust on the Moravo-Silesian foreland and only later affected by the N–S trending Moldanubian Thrust. Also, paleomagentic studies (e.g. Krs et al., 1995) show unequivocal evidence for rotation of the Moravo-Silesian Belt to the SE of the Moldanubian Thrust, which has been rotated clockwise through at least 90o (with respect to the Rhenohercynian Belt in Germany) since the Devonian.

The high velocity lower crust beneath the Bohemian Massif (velocities within the range of 6.8–7.8 km s^{-1} over a depth range of 28–40 km) terminates at 575 km along the profile. It is in contrast with the Moho in the Fore-Sudetic Monocline interpreted as the first-order discontinuity at 30 km depth. If we think of the gradient zone of the lower crust as a characteristic feature of the Bohemian Massif in this area, then the termination of the high velocity lower crust can be considered as a north-eastern termination of the Bohemian Massif at a crust/mantle level affected by eastward collisional tectonics and probably also rotation.

8.4. Fore-Sudetic Monocline and TESZ

The northern Variscan foreland represented by the TESZ has a structure that corresponds to the previous studies (Grad et al., 2002; Środa et al., 2006; Grad et al., in press). The upper crust of the Fore-Sudetic Monocline has slightly different velocity than that of the Bohemian Massif (Fig. 4). But it has noticeably different crust from that of the Mid-Polish Trough and thus it most probably belongs to the Variscan orogen. Compared to the Bohemian Massif, the area of the Fore-Sudetic Monocline displays considerably lower velocities in the upper crust beyond a distance of 600 km along the profile. There, the Lower Paleozoic metamorphic basement is overlain by largely flat lying

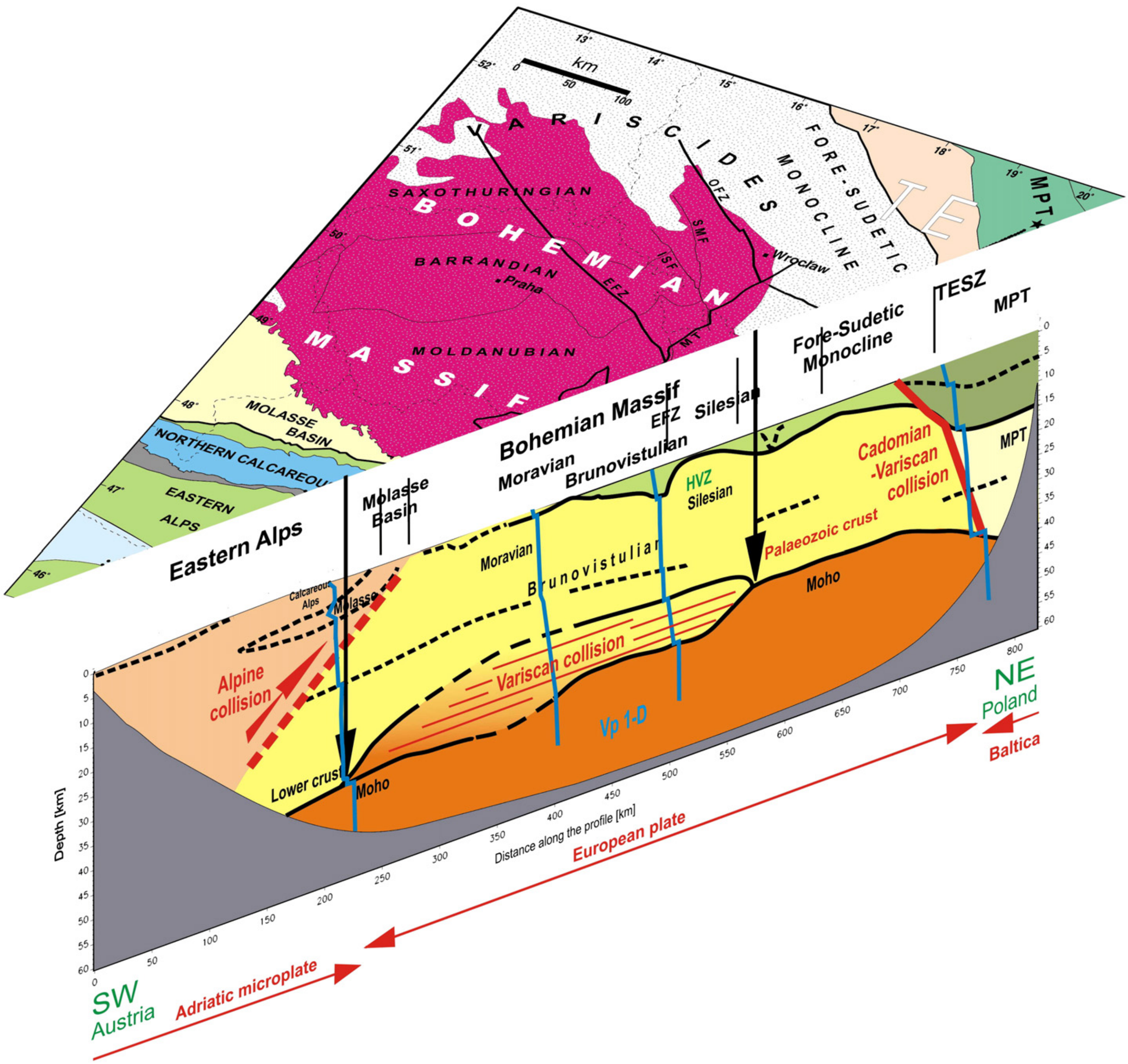

Fig. 12. Schematic geological/tectonic representation along joint profile CEL10 and ALP04 with simplified tectonic map. Black vertical arrows mark the extension of the lower crustal gradient zone of the Bohemian Massif at the surface. Superimposed, there are 1-D velocity characteristics for different parts of the profile: Eastern Alps, Moravian, Silesian, TESZ. Vertical exaggeration is 1:4. EFZ, Elbe Fault Zone; MPT, Mid-Polish Trough; HVZ, high velocity zone; TESZ, Trans-European Suture Zone.

sedimentary rocks with velocities of 3.7–5.3 km s^{-1} to the depths of 3–6 km. Underneath this cover, the upper crust has relatively low P-wave velocities of 5.9–6.05 km s^{-1}. Similar upper crustal velocities were also found in the Paleozoic part of the P1 and P4 profiles (Guterch et al., 1986; Jensen et al., 1999). Dadlez et al. (2005) showed that in the Variscan Belt the lower crust has velocities of 6.5–6.6 km s^{-1} and the middle crust is in the range of 6.2–6.3 km s^{-1}, which corresponds to the velocity range detected from our data beneath the Fore-Sudetic Monocline. Further to the NE, the velocities of 3.6–5.5 km s^{-1} at the depths of 15 km correspond to Permian to Mesozoic sediments and low-grade metasediments of the Mid-Polish Trough, as well as to older metasedimentary sequences. Similar low velocities (<6.4 km s^{-1}) to the depths of about 20 km are observed on several other seismic profiles in the TESZ area, e.g. Grad et al. (2002).

The Moho in the Fore-Sudetic Monocline is interpreted as a first-order discontinuity with a velocity jump from 6.7 to 7.9–8.0 km s^{-1} at a depth of 30 km and is in sharp contrast with the high velocity lower crust of the Bohemian Massif. The deepening of the Moho towards the axial zone of the TESZ, the Mid-Polish Trough, to the depth of about 40 km is in agreement with other investigations of the TESZ as a transition zone between the Paleozoic Platform and the East European Craton (e.g., Grad et al., 2003a; Grad et al., 2007). There are still debates on the location of the boundary between the internal and external Variscides, which is supposed to be somewhere in the Fore-Sudetic Monocline between 620 and 650 km along the profile (e.g., Mazur et al., 2006). Some authors, e.g. Franke and Żelaźniewicz (2002), consider continuation of the Silesian as far as the Krakow–Lubliniec Zone where the contact of the Silesian and the Fore-Sudetic Monocline is located on the surface. Our results do not help in answering these questions, as there is no differentiation in the seismic model observed in this area.

9. Summary and conclusions

High quality seismic data were acquired during the CELEBRATION 2000 and ALP 2002 experiments along 820 km long, SW–NE striking profile at the easternmost margin of the Variscan belt and on the contact with the Alps and Baltica. The data have been interpreted by tomographic inversion of the first arrival travel times and by two-dimensional ray-tracing of the first and later arrivals, as well as by calculation of synthetic seismograms for the P-wave arrivals. Our effort to model these data provides us with the conclusions that are summarized in Fig. 12. We show differentiation of the structure both in the upper crustal parts and also at lower crust and upper mantle levels, which gives some indications for tracing of crust-forming processes during the Variscan and Alpine orogeny.

In the SW, the N–S directed Tertiary orogeny resulted in northward thrusting of the Eastern Alpine nappes along the northern rim of the Alps. The interpretation of joint ALP04 and CEL10 models shows the lower velocities of the Molasse and Helvetic Flysch sediments detectable not only on the surface but dipping SW below the Alpine nappes, where they alternate with higher velocities of the thick carbonatic layers of the Northern Calcareous Alps. Beneath the Eastern Alps, the crust thickens and the south-westward dip of the Moho continues to reach the maximum thickness of 40–44 km closer to the axis of the Eastern Alps. This reflects the thickening of the crust in a consequence of large-scale collision of the Adriatic and European plates during the Tertiary.

The eastern margin of the Bohemian Massif, represented by the Moravo-Silesian zone, provides a detailed picture of geological inventory as a zone of sheared and metamorphosed Brunia-derived rocks. These rocks emerge through the Moravo-Silesian in the tectonic windows along the deformation zone, the Moldanubian Thrust. Three orogenic cycles in this area, the lowermost cycle represented by the Pan-African (Cadomian) Brunovistulian foreland terrane, the Variscan accretion wedge and the Alpine accretion wedge, influenced the tectonic development. The lower crust in this area is characterized by high velocities with no distinct Moho interface. The high velocity gradient lower crust seems to be a characteristic feature of the Moravo-Silesian overthrust by the Moldanubian unit. Slightly different properties of the crust in the Moravian and Silesian units might be attributed to the variation in distance from the Moldanubian Thrust front as well as the different type of contact of the Brunia with the Moldanubian and its northern root sector and thus resulting in different degree of metamorphism and/or deformation during tectonic processes. The north-eastern termination of the high velocity lower crust in the Bohemian Massif could be seen as the termination of the Variscan collision tectonics on a crust/mantle level.

Lower velocities in the upper crust in the Fore-Sudetic Monocline represent the Lower Paleozoic metamorphic basement overlain by largely flat lying sedimentary rocks. The Moho in the Fore-Sudetic Monocline interpreted as a first-order discontinuity is in a sharp contrast with the high velocity lower crust of the Bohemian Massif. It might reflect different tectonic regime compared to the eastern Bohemian Massif. The deepening of the Moho towards the axial zone of the TESZ, the Mid-Polish Trough, to the depth of about 40 km is in agreement with other investigations of the TESZ as a transition zone between the Paleozoic Platform and the East European Craton.

Acknowledgements

The CELEBRATION 2000 and ALP 2002 projects were supported by the Ministry of Environment of the Czech Republic, by the Polish State Committee for Scientific Research, the Ministry of the Environment of Poland, the Polish Oil and Gas Company, the Association for Deep Geological Investigations in Poland (ADGIP), and Austrian Academy of Sciences. The other sponsors were the Geological Survey and the Academy of Sciences of Slovakia, the Eötvös Loránd Geophysical Institute in Hungary, Austrian Academy of Sciences and the U. S. National Science Foundation (NSF). Seismic stations were provided by the University of Texas at El Paso, USA, IRIS/Passcal consortium, and GeoForschungsZentrum Potsdam, Germany. Seismic data processing has been performed with Seismic Unix software (Cohen and Stockwell, 1997). GMT software (Wessel and Smith, 1995) has been used for plotting maps and tomographic results. We thank Dr. J. Hole for providing us with his inversion code. The authors are also grateful to two anonymous reviewers and Hans Thybo for their valuable comments.

References

Aichroth, B., Prodehl, C., Thybo, H., 1992. Crustal structure along the Central Segment of the EGT from seismic-refraction studies. Tectonophysics 207, 43–64.

Aki, K., Richards, P.G., 1980. Quantitative seismology, theory and methods. Columbia University.

Behm, M., Brückl, E., Chwatal, W., Tybo, H., 2007. Application of stacking and inversion techniques to three-dimensional wide-angle reflection and refraction seismic data of the Eastern Alps. Geophys. J. Int. 170 (1), 275–298. doi:10.1111/j.1365-246X.2007.03393.x.

Belka, Z., Ahrendt, H., Franke, W., Wemmer, K., 2000. The Baltica–Gondwana suture in central Europe: evidence from K-Ar ages of detrital muscovites and biogeographic data. In: Franke, W., Haak, V., Oncken, O., Tanner, D. (Eds.), Orogenic Processes: Quantification and Modelling in the Variscan Belt. Geol. Soc., London, Spec. Publ., vol. 179, pp. 87–102.

Belka, Z., Valverde-Vaquero, P., Ahrendt, H., Wemmer, K., Franke, W., Schäffer, J., 2002. Accretion of first Gondwana derived terranes at the margin of Baltica. In: Winchester, J.A., Pharaoh, T.C., Verniers, J. (Eds.), Paleozoic Amalgamation of Central Europe. Geol. Soc., London, Spec. Publ., vol. 201, pp. 19–36.

Beránek, B., Zátopek, A., 1981. Earth's crust structure in Czechoslovakia and Central Europe by methods of explosion seismology. In: Zátopek, A. (Ed.), Geophysical Synthesis in Czechoslovakia. Veda, Bratislava.

Beránek, B., Zounková, M., 1977. Investigations of the Earth's crust in Czechoslovakia using industrial blasting. Stud. Geophys. Geod. 21, 273–280.

Berthelsen, A., 1992. From Precambrian to Variscan Europe. In: Blundell, D.J., Freeman, R., Muller, S. (Eds.), A Continent Revealed—The European Geotraverse. Cambridge Univ. Press, New York, pp. 153–164.

Bielik, M., Šefara, J., Kováč, M., Bezák, V., Plašienka, D., 2004. The Western Carpathians—interaction of Hercynian and Alpine processes. Tectonophysics 393, 63–86.

Bleibinhaus, F., Gebrande, H., 2006. Crustal structure of the Eastern Alps along the TRANSALP profile from wide-angle seismic tomography. Tectonophysics 414 (1–4), 51–69. doi:10.1016/j.tecto.2005.10.028.

British Institutions Reflection Profiling Syndicate (BIRPS) and Étude Continentale et Océanique par Réflexion et Refraction (ECORS), 1986. Deep seismic reflection profiling between England, France and Ireland. J. Geol. Soc. London 143, 45–52.

Brückl, E., Bodoky, T., Hegedüs, E., Hrubcová, P., Gosar, A., Grad, M., Guterch, A., Hajnal, Z., Keller, G.R., Špičák, A., Sumanovac, F., Thybo, H., Weber, F., ALP 2002 Working Group, 2003. ALP 2002 seismic experiment. Stud. Geophys. Geod. 47, 671–679.

Brückl, E., Bleibinhaus, F., Gosar, A., Grad, M., Guterch, A., Hrubcová, P., Keller, G.R., Majdański, M., Sumanovac, F., Tiira, T., Yliniemi, J., Hegedus, E., Thybo, H., 2007. Crustal structure due to collisional and escape tectonics in the Eastern Alps region based on profiles Alp01 and Alp02 from the ALP 2002 seismic experiment. J. Geophys. Res. 112, B06308. doi:10.1029/2006JB004687.

Carbonell, R., Simancas, F., Juhlin, C., Pous, J., Pérez-Estaún, A., Gonzalez-Lodeiro, F., Muñoz, G., Heise, W., Ayarza, P., 2004. Geophysical evidence of a mantle derived intrusion in SW Iberia. Geophys. Res. Lett. 31, L11601. doi:10.1029/2004GL019684.

Červený, V., Pšenčík, I., 1984. SEIS83 — numerical modelling of seismic wave fields in 2-D laterally varying layered structures by the ray method. In: Engdal, E.R. (Ed.), Documentation of Earthquake Algorithms. Rep. SE-35, World Data Cent. A for Solid Earth Geophysics, Boulder, Colo. , pp. 36–40.

Christensen, N.I., Mooney, W.D., 1995. Seismic velocity structure and composition of the continental crust: a global view. J. Geophys. Res. 100, 9761–9877.

Cohen, J.K., Stockwell Jr., J.W., 1997. CWP/SU: Seismic Unix Release 30: a free package for seismic research and processing. Center for Wave Phenomena, Colorado School of Mines.

Dadlez, R., Grad, M., Guterch, A., 2005. Crustal structure below the Polish Basin: is it composed of proximal terranes derived from Baltica? Tectonophysics 411, 111–128.

Dallmeyer, R.D., Urban, M., 1994. Evolution of Variscan (Hercynian) and comparable Palaeozoic orogenic belts. J. Czech Geol. Soc. 39, 21–22.

Dallmeyer, D., Franke, W., Weber, K. (Eds.), 1995. Pre-Permian Geology of Central and Eastern Europe. Springer, New York.

Deutches Kontinentales Reflektionsseismisches Programm (DEKORP) Research Group, 1985. First results and preliminary interpretation of deep-reflection seismic recording along profile DEKORP 2-South. J. Geophys. 57, 137–165.

Deutches Kontinentales Reflektionsseismisches Programm (DEKORP) Research Group, 1988. Results of the DECORP 4/KTB Oberpfalz deep seismic reflection investigation. J. Geophys. 62, 69–101.

Dudek, A., 1980. The Crystalline Basement Block of the Outer Carpathians in Moravia-Brunovistulicum. Rozpravy Československé Akademie věd, Řada matematika-přírodní vědy, vol. 90, pp. 85–90.

Edel, J.B., Schulmann, K., Holub, F.V., 2003. Anticlockwise and clockwise rotations of the Eastern Variscides accommodated by dextral lithospheric wrenching: paleomagnetic and structural evidence. J. Geol. Soc. London 160, 209–218.

Finger, F., Hanzl, P., Pin, C., von Quadt, A., Steyrer, H.P., 2000. The Brunovistulian: Avalonian Precambrian sequence at the eastern end of the Central European Variscides? In: Franke, W., Haak, V., Oncken, O., Tanner, D. (Eds.), Orogenic Processes: Quantification and Modelling in the Variscan Belt. Geol. Soc., London, Spec. Publ., vol. 179, pp. 103–112.

Franke, W., 2006. The Variscan orogen in Central Europe: construction and collapse. Geol. Soc. London, Memoirs 32 (1), 333–343.

Franke, W., Żelaźniewicz, A., 2002. Structure and evolution of the Bohemian Arc. In: Winchester, J.A., Pharaoh, T.C., Verniers, J. (Eds.), Paleozoic Amalgamation of Central Europe. Geol. Soc., London, Spec. Publ., vol. 201, pp. 279–293.

Franke, W., Haak, V., Oncken, O., Tanner, D. (Eds.), 2000. Orogenic Processes: Quantification and Modelling in the Variscan Belt. Geol. Soc., London, Spec. Publ., vol. 179.

Fritz, H., Dallmeyer, R.D., Neubauer, F., 1996. Thick-skinned versus thin-skinned thrusting: rheology controlled thrust propagation in the Variscan collisional belt (the south-eastern Bohemian Massif, Czech Republic–Austria). Tectonics 15, 1389–1413.

Furlong, K.P., Fountain, D.M., 1986. Continental crustal underplating: thermal considerations and seismic–petrologic consequences. J. Geophys. Res. 91, 8285–8294.

Gee, D.G., Zeyen, H. (Eds.), 1996. EUROPROBE 1996 — Lithosphere Dynamics. Origin and Evolution of Continents. . EUROPROBE Secretariat. Uppsala University.

Giese, P., Prodehl, C., 1976. In: Giese, P., Prodehl, C., Stein, A. (Eds.), Main Features of Crustal Structures in the Alps, in Explosion Seismology in Central Europe. Springer, Berlin, pp. 347–363.

Grad, M., Keller, G.R., Thybo, H., Guterch, A., POLONAISE Working Group, 2002. Lower lithospheric structure beneath the Trans-European suture zone from POLONAISE'97 seismic profiles. Tectonpophysics 360, 153–168.

Grad, M., Jensen, S.L., Keller, G.R., Guterch, A., Thybo, H., Janik, T., Tiira, T., Yliniemi, J., Luosto, U., Motuza, G., Nasedkin, V., Czuba, W., Gaczyński, E., Środa, P., Miller, K.C., Wilde- Piórko, M., Komminaho, K., Jacyna, J., Korabliova, L., 2003a. Crustal structure of the Trans- European suture zone region along POLONAISE'97 seismic profile P4. J. Geophys. Res. 108 (B11), 2541. doi:10.1029/2003JB002426.

Grad, M., Špičák, A., Keller, G.R., Guterch, A., Brol, M., Hegedfls, E., SUDETES Working Group, 2003b. SUDETES 2003 seismic experiment. Stud. Geophys. Geod. 47, 681–689. doi:10.1023/ A:1024732206210.

Grad, M., Guterch, A., Polkowska-Purys, A., 2005. Crustal structure of the Trans-European Suture Zone in Central Poland — reinterpretation of the LT-2, LT-4 and LT-5 deep seismic sounding profiles. Geol. Quart. 49 (3), 243–252.

Grad, M., Guterch, A., Keller, G.R., POLONAISE'97 and CELEBRATION 2000 Working Groups, 2007. Variations in lithospheric structure across the margin of Baltica in Central Europe and the role of the Variscan and Carpathian orogenies. In: Hatcher Jr., R.D., Carlson, M.E., McBride, J.H., Martinez Catalán, J.R. (Eds.), 4-D Framework of Continental Crust. Geological Society of America Memoir, vol. 200, pp. 341–356. doi:10.1130/2007.1200(17).

Grad, M., Guterch, A., Mazur, S., Keller, G.R., Špičák, A., Hrubcová, P., Geissler, W.H., SUDETES 2003 Working Group (in press), Lithospheric structure of the Bohemian Massif and adjacent Variscan belt in central Europe based on Profile S01 from the SUDETES 2003 experiment, J. Geophys. Res., doi: 2007JB005497RR.

Gruntorád, J., Lhotská, Z., 1973. Geophysical research into neovolcanic rocks of the Nízký Jeseník Mts. (in Czech). Geophysical Survey in the Jeseníky Mts. Charles University, Prague, pp. 56–74.

Grygar, R., Gnojek, I., Hubatka, F., Jelínek, J., 2002. Brunovistulian Terrane — synthesis of morphostructural analysis and geophysical data (Moravo-Silesian Area, Czech Republic). Geolines 14, 26–27.

Guterch, A., Grad, M., Materzok, R., Perchuć, E., 1986. Deep structure of the Earth's crust in the contact zone of the Palaeozoic and Precambrian Platforms in Poland (Tornquist–Teisseyre Zone). Tectonophysics 128, 251–279.

Guterch, A., Grad, M., Thybo, H., Keller, G.R., POLONAISE Working Group, 1999. POLONAISE'97 — international seismic experiment between Precambrian and Variscan Europe in Poland. Tectonpophysics 314, 101–121.

Guterch, A., Grad, M., Keller, G.R., Posgay, K., Vozár, J., Špičák, A., Brueckl, E., Hajnal, Z., Thybo, H., Selvi, O., CELEBRATION 2000 Experiment Team, 2003. CELEBRATION 2000 Seismic Experiment. Stud. Geophys. Geod. 47, 659–670.

Handy, M.R., Streit, J.E., 1999. Mechanics and mechanism of magmatic unerplating: inferences from mafic veins in deep crustal mylonite. Earth Planet. Sci. Lett. 165, 271–286.

Hole, J.A., 1992. Non-linear high-resolution three-dimensional seismic travel time tomography. J. Geophys. Res. 97, 6553–6562.

Hrubcová, P., Środa, P., Špičák, A., Guterch, A., Grad, M., Keller, R., Brückl, E., Thybo, H., 2005. Crustal and uppermost mantle structure of the Bohemian Massif based on data from CELEBRATION 2000 experiment. J. Geophys. Res. 110, B11305. doi:10.1029/2004JB003080.

Hubatka, F., Švancara, J., 2002a. Geologicko-geofyzikální model zemské kůry v místě křížení profilů 8HR/85 a CEL10. Internal Report, Archive of the Geophysical Institute ASCR, in Czech. .

Hubatka, F., Švancara, J., 2002b. Geologicko-geofyzikální model zemské kůry v místě křížení profilů KII a CEL10. Internal Report, Archive of the Geophysical Institute ASCR, in Czech.

Humphreys, E., Clayton, R.W., 1988. Adaptation of backprojection tomography to seismic travel time problems. J. Geophys. Res. 93, 1073–1085.

Hurich, C.A., Deemer, S.J., Indares, A., Salisbury, M., 2001. Compositional and metamorphic controls on velocity and reflectivity in the continental crust: an example from the Grenville Province of eastern Québec. J. Geophys. Res. 106, 665–682.

Janik, T., Yliniemi, J., Grad, M., Thybo, H., Tiira, T., POLONAISE P2 Working Group, 2002. Crustal structure across the TESZ along POLONAISE'97 seismic profile P2 in NW Poland. Tectonophysics 360, 129–152.

Jensen, S.L., Janik, T., Thybo, H., POLONAISE'97 Working Group, 1999. Seismic structure of the Palaeozoic platform along POLONAISE'97 profile P1 in southwestern Poland. Tectonophysics 314, 123–143.

Komminaho, K., 1997. Software manual for programs MODEL and XRAYS — graphical interface for SEIS83 Program package. Rep. 20, 31, pp Dept. of Geophys., Univ. of Oulu, Oulu, Finland.

Krs, M., Krsová, M., Pruner, P., 1995. Paleomagnetism and paleogeography of Variscan formations of the Bohemian Massif: a comparison with other regions in Europe. Stud. Geophys. Geod. 39, 309–319.

Majdański, M., Grad, M., Guterch, A., SUDETES 2003 Working Group, 2006. 2-D seismic tomographic and ray tracing modelling of the crustal structure across the Sudetes Mountains basing on SUDETES 2003 experiment data. Tectonophysics 413, 249–269. doi:10.1016/j.tecto.2005.10.042.

Majdański, M., Kozlovskaya, E., Grad, M., SUDETES 2003 Working Group, 2007. 3D structure of the Earth's crust beneath the northern part of the Bohemian Massif. Tectonophysics 437, 17–36. doi:10.1016/j.tecto.2007.02.015.

Majerová, M., Novotný, M., (1986), Výzkum zemské kůry pomocí hlubinné sondáže. In: Geofyzikální model litosféry, eds. M. Blížkovský, MS Geofyzika n.p. Brno, GFÚ ČSAV Praha, GFÚ SAV Bratislava, in Czech.

Málek, J., Brož, M., Fischer, T., Horálek, J., Hrubcová, P., Janský, J., Novotný, O., Růžek, B., 2001. Seismic measurements along short profiles in western Bohemia during the Celebration 2000 experiment. Acta Mont., A 18 (121), 15–28.

Malinowski, M., Żelaźniewicz, A., Grad, M., Guterch, A., Janik, T., CELEBRATION Working Group, 2005. Seismic and geological structure of the crust in the transition from Baltica to Palaeozoic Europe in SE Poland — CELEBRATION 2000 experiment, profile CEL02. Tectonophysics 401, 55–77. doi:10.1016/j.tecto.2005.03.011.

Matte, P., 1986. Tectonics and plate tectonic model for the Variscan Belt of Europe. Tectonophysics 126, 329–374.

Matte, Ph., 1991. Accretionary history and crustal evolution of the Variscan belt in Western Europe. Tectonophysics 196, 309–337.

Matte, Ph., 2001. The Variscan collage and orogeny (480–290 Ma) and the tectonic definition of the Armorica microplate: a review. Terra Nova 13, 122–128.

Matte, Ph., Maluski, H., Rajlich, P., Franke, W., 1990. Terrane boundaries in the Bohemian Massif: Result of large-scale Variscan shearing. Tectonophysics 177, 151–170.

Mazur, S., Alexandrowski, P., Krysza, R., Oberc-Dziedzicz, T., 2006. The Variscan Orogen in Poland. Geol. Quart. 50 (1), 89–118.

Morozov, I.B., Smithson, S.B., Chen, J., Hollister, L.S., 2001. Generation of new continental crust and terrane accretion in Southeastern Alaska and Western British Columbia: constraints from P- and S-wave wide-angle seismic data (ACCRETE). Tectonophysics 341, 49–67.

Mueller, H.J., 1995. . Modelling of the lower crust by simulation of the in situ conditions: an example from Saxonian Erzgebirge. Phys. Earth Planet. Inter. 92, 3–15.

Oliver, G.J.H., Corfu, F., Krogh, T.E., 1993. U-Pb ages from SW Poland: evidence for a Caledonian suture zone between Baltica and Gondwana. J. Geol. Soc. London 150, 355–369.

Onken, O., Plesh, A., Weber, J., Ricken, W., Schrader, S., 2000. Passive margin detachment during arc–continent collision (central European Variscides). In: Franke, W., et al. (Ed.), Orogenic Processes: Quantification and Modelling in the Variscan Belt. Geol. Soc. Spec. Publ., vol. 179, pp. 9–20.
Plomerová, J., Babuška, V., Ruprechtová, L., 1984. Velocities of seismic waves propagating through the Bohemian Massif from foci in Poland. Stud. Geophys. Geod. 28, 56–66.
Reinecker, J., Lenhardt, W., 1999. Present-day stress field and deformation in eastern Austria. Int. J. Earth Sci. 88, 532–550.
Růžek, B., Vavryčuk, V., Hrubcová, P., Zedník, J., CELEBRATION Working Group, 2003. Crustal anisotropy in the Bohemian Massif, Czech Republic: observations based on the Central European Lithospheric Experiment Based on Refraction (CELEBRATION) 2000. J. Geophys. Res. 108 (B8), 2392. doi:10.1029/2002JB002242.
Schulmann, K., Gayer, R., 2000. A model for a continental accretionary wedge developed by oblique collision: the NE Bohemian Massif. J. Geol. Soc. London 157, 401–416.
Schulmann, K., Kröner, A., Hegner, E., Wendt, I., Konopásek, J., Lexa, O., Štipská, P., 2005. Chronological constraints on the pre-orogenic history, burial and exhumation of deep- seated rocks along the Eastern Margin of the Variscan Orogen, Bohemian Massif, Czech Republic. Am. J. Sci. 305, 407–448.
Schulmann, K., Lexa, O., Štípská, P., Racek, M., Tajčmanová, L., Konopásek, J., Edel, J.B., Peschler, A., Lehmann, J., 2008. Vertical extrusion and horizontal channel flow of orogenic lower crust: key exhumation mechanisms in large hot orogens? J. Metamorph. Geol. 26, 273–297. doi:10.1111/j.1525- 1314.2007.00755.x.
Simancas, J.F., Carbonell, R., González Lodeiro, F., Pérez Estaún, A., Juhlin, C., Ayarza, P., Kashubin, A., Azor, A., Martínez Poyatos, D., Almodóvar, G.R., Pascual, E., Sáez, R., Expósito, I., 2003. Crustal structure of the transpressional Variscan orogen of SW Iberia: SW Iberia deep seismic reflection profile (IBERSEIS). Tectonics 22 (6), 1062. doi:10.1029/2002TC001479.
Špaček, P., Sýkorová, Z., Pazdírková, J., Švancara, J., Havíř, J., 2006. Present-day seismicity of the south-eastern Elbe Fault System (NE Bohemian Massif). Stud. Geophys. Geod. 50, 233–258.
Środa, P., Czuba, W., Grad, M., Guterch, A., Tokarski, A.K., Janik, T., Rauch, M., Keller, G.R., Hegedüs, E., Vozár, J., CELEBRATION 2000 Working Group, 2006. Crustal and upper mantle structure of the Western Carpathians from CELEBRATION 2000 profiles CEL01 and CEL04: seismic models and geological implications. Geophys. J. Int. 167, 737–760. doi:10.1111/j.1365-246X.2006.03104.x.
Tait, J.A., Schätz, M., Bachtadse, V., Soffel, H., 2000. Palaeomagnetism and Paleozoic palaeogeography of Gondwana and European terranes. In: Franke, W., Haak, V., Oncken, O., Tanner, D. (Eds.), Orogenic Processes: Quantification and Modelling in the Variscan Belt. Geol. Soc. Spec. Publ., vol. 179, pp. 21–34.
Thybo, H., Janik, T., Omelchenko, V.D., Grad, M., Garetsky, R.G., Belinsky, A.A., Karatayev, G.I., Zlotski, G., Knudsen, M.E., Sand, R., Yliniemi, J., Tiira, T., Luosto, U., Komminaho, K., Giese, R., Guterch, A., Lund, C.E., Kharitonov I, O.M., Ilchenko, T., Lysynchuk, D.V., Skobelev, V.M., Doody, J.J., 2003. Upper lithospheric seismic velocity structure across the Pripyat Trough and the Ukrainian Shield along the EUROBRIDGE'97 profile. Tectonophysics 371, 41–79.
Vavryčuk, V., Hrubcová, P., Brož, M., Málek, J., ALP 2002 Working Group, 2004. Azimuthal variation of Pg velocity in the Moldanubian, Czech Republic: observations based on a multi-azimuthal common-shot experiment. Tectonophysics 387/1–4, 189–203. doi:10.1016/j.tecto.2004.06.015.
Vidale, J.E., 1990. Finite-difference calculation of travel times in three dimensions. Geophysics 55, 521–526.
Wessel, P., Smith, W.H.F., 1995. New version of Generic Mapping Tools released. Eos Trans. AGU 76, 329.
Wilde-Piórko, M., Saul, J., Grad, M., 2005. Differences in the crustal and uppermost mantle structure of the Bohemian Massif from teleseismic receiver functions. Stud. Geophys. Geod. 49, 85–107.
Winchester, J.A., Pharaoh, T.C., Verniers, J., 2002. Paleozoic Amalgamation of Central Europe. J. Geol. Soc. London, Spec. Publ., vol. 201.
Winchester, J.A., Pharaoh, T.C., Verniers, J., Ioane, D., Seghedi, A., 2006. Palaeozoic accretion of Gondwana-derived terranes to the East European Craton: recognition of detached terrane fragments dispersed after collision with promontories. J. Geol. Soc. London, Memoirs 32 (1), 323–332.
Zelt, C.A., 1994. ZPLOT — an interactive plotting and picking program for seismic data. Bullard Lab. Univ. of Cambridge, Cambridge UK.